



Investigating the Role of CBX2 to Promote Cell Growth in Triple Negative Breast Cancer

By

Lucie Bilton

201707061

Supervisor: Dr Mark Wade

Second supervisor: Dr Dan Hampshire

MSc by Research in Biomedical Science

November 2022

## Abstract

Breast cancer is the uncontrolled proliferation of breast cells and is one of the most common cancers in the UK. It is a complex disease that can be divided into different subtypes based upon the presence or lack of hormone receptors, namely the oestrogen receptor (ER), progesterone receptor (PR) and human epidermal factor receptor 2 (HER2). Breast cancer without hormone receptor expression is called basal-like or triple negative breast cancer (TNBC). TNBC is more aggressive, and patients tend to have a poor prognosis partly due to a lack of targeted treatment. The identification of new therapeutic options for TNBC is therefore needed.

Dysregulated epigenetic control of the chromatin state, and therefore gene expression, via aberrant chemical modification of histone proteins can play an important role in cancer progression. Previous studies have shown that the epigenetic regulatory protein, CBX2, which modulates histone ubiquitination and repression of gene expression, is implicated in breast cancer development. The aim of this study was to investigate the role of CBX2 and its effect on cell growth in TNBC using the TNBC cell lines MDA-MB-231 and MDA-MB-468, to help determine whether CBX2 is a viable potential therapeutic target for TNBC.

In this study we showed successful knockdown of CBX2 in both TNBC cell lines using small interfering RNAs (siRNAs). We showed that expression of the tumour suppressor protein RBL2 was upregulated after CBX2 knockdown, suggesting CBX2 represses the expression of RBL2. RBL2 is a member of the DREAM complex which prevents progression through the cell cycle via inhibition of key cell cycle genes. Gene expression profiling showed that CBX2 knockdown increased *RBL2* expression and reduced the expression of RBL2 target genes (*PLK1*, *AURKA*, *CCNA2*, *CDK1*). Chromatin immunoprecipitation (ChIP) showed that CBX2 knockdown increased enrichment of RBL2 at DREAM complex target sites, therefore demonstrating that CBX2 plays a role in promoting cell growth and proliferation via repression of DREAM complex activity. This study adds insight into the mechanisms by which CBX2 promotes progression of TNBC and shows the potential of CBX2 as a new therapeutic target.



## Acknowledgements

I would like to thank Dr Mark Wade for being a fantastic supervisor and allowing me to complete this project in his lab. His support, knowledge, good words of advice and belief in me have really helped me to complete this project.

I would like to thank Antonia Barry and Quentin Rodriguez-Barucg for their support, encouragement, kindness and help in the laboratory.

I would like to thank my friends and family who have consistently supported me and believed in me no matter what. I am grateful for the support from them that helped me through the past year.

## Publications to date

### **PEER REVIEWED PUBLICATIONS:**

Bilton, L., Warren, C., Humphries, R., Kalsi, S., Waters, E., Francis, T., Dobrowinski, W., Beltran-Alvarez, P. and Wade, M., 2022. The Epigenetic Regulatory Protein CBX2 Promotes mTORC1 Signalling and Inhibits DREAM Complex Activity to Drive Breast Cancer Cell Growth. *Cancers*, 14(14), p.3491.

# Contents

Abstract.....	i
Acknowledgements.....	iii
Publications to date.....	iv
List of Figures.....	ix
List of Tables.....	x
Abbreviation List.....	xi
Chapter 1 Background.....	15
1.1 Cancer.....	15
1.2 Breast Cancer.....	16
1.2.1 Triple negative breast cancer.....	18
1.3 Epigenetics.....	20
1.3.1 Chromatin.....	20
1.3.2 Histone post-translational modifications (PTMs).....	20
1.3.3 Dysregulation of histone modifications and cancer.....	22
1.4 Polycomb Repressive Complex 1 (PRC1).....	22
1.5 CBX2.....	24
1.5.1 CBX2 and breast cancer.....	25
1.6 RBL2 and E2F4.....	26
1.7 Thesis Aims.....	28
1.7.1 Hypothesis.....	28
1.7.2 Aims.....	28
1.7.3 Ethical Considerations.....	28
Chapter 2. Materials and Methods.....	29
2.1 Cell Culture.....	29
2.2 Trypsinisation.....	29
2.3 Counting cells.....	29

2.4 Cell Transfection.....	30
2.5 Cell count assay .....	31
2.6 Sulforhodamine B (SRB) Assay .....	32
2.7 Western Blot Analysis .....	32
2.7.1 Protein lysis.....	32
2.7.2 Bicinchoninic acid (BCA) assay .....	33
2.7.3 Gel Electrophoresis .....	34
2.7.4 Protein Transfer .....	35
2.7.5 Immunoblotting .....	36
2.8 Gene Expression Analysis.....	39
2.8.1 RNA Extraction .....	39
2.8.2 Reverse Transcription (RT).....	39
2.8.3 Quantitative Polymerase Chain Reaction (qPCR) .....	39
2.9 Co-Immunoprecipitation (Co-IP).....	43
2.10 Chromatin Immunoprecipitation (ChIP).....	44
2.10.1 Plating of Cells.....	44
2.10.2 Formaldehyde Fixation .....	44
2.10.3 Cell lysis and sonication.....	45
2.10.4 Binding of antibody to magnetic beads .....	46
2.10.5 Elution and cross-link reversal .....	47
2.10.6 Protein and RNA digestion .....	47
2.10.7 DNA Purification .....	48
2.11 Cleavage Under Targets & Release Using Nuclease (CUT & RUN) .....	48
2.11.1 Cell Preparation and Binding of Primary Antibody .....	49
2.11.2 Binding of pAG-MNase Enzyme .....	50
2.11.3 DNA Digestion and Diffusion.....	50
2.11.4 Preparation of the Input Sample .....	51

2.11.5 DNA Purification .....	51
2.11.6 Qubit DNA quantification .....	52
Chapter 3 Results.....	53
3.1 Knockdown of CBX2 reduces cell growth in the MDA-MB-468 cell line .....	53
3.2 Gene expression profiling after CBX2 knockdown in MDA-MB-468 cells.....	55
3.3 RBL2 and E2F4 protein expression after CBX2 knockdown in MDA-MB-231 and MDA-MB-468 cells.....	57
.....	58
.....	59
3.4 Gene expression profiling shows that knockdown of CBX2 affects RBL2 target genes in MDA-MB-468 cells .....	60
3.5 RBL2 and E2F4 co-immunoprecipitation following CBX2 knockdown on MDA-MB- 468 cells .....	62
3.6 Enrichment of <i>RBL2</i> at RBL2 target gene promoters following knockdown of CBX2 in MDA-MB-231 cells.....	64
3.7 Enrichment of <i>RBL2</i> at RBL2 target gene promoters following the knockdown of <i>CBX2</i> in MDA-MB-468 cells .....	66
3.8 Determining CBX2 chromatin interactions via CUT & RUN sequencing .....	68
3.8.1 Quality Control analysis of Cut & Run-sequencing .....	70
Chapter 4 Discussion.....	72
4.1 CBX2 knockdown causes reduced cell growth .....	72
4.2 RBL2 expression is upregulated after the knockdown of CBX2 and there is no effect on E2F4 .....	73
4.3 Formation of DREAM complex after CBX2 knockdown.....	74
4.4 CBX2 knockdown increases gene expression of RBL2 and affects RBL2 target genes .....	75
4.5 CBX2 knockdown increases RBL2 enrichment at DREAM complex target sites .....	75
4.6 CUT & RUN to further understand CBX2 chromatin interactions on the genome .....	77

4.7 Conclusion .....	79
Future Directions .....	80
References .....	82

## List of Figures

Figure 1.1 Percentage of the 4 most common cancers vs other cancers.....	16
Figure 1.2 Chromatin Structure.....	21
Figure 1.3 PRC1 and PRC2.....	24
Figure 2.1 Field on haemocytometer used to count cells.....	30
Figure 3.1 Relative cell counts in MDA-MB-468 cells following CBX2 knockdown.....	54
Figure 3.2 SRB assay following the knockdown of CBX2 in MDA-MB-468 cells.....	55
Figure 3.3 Gene expression profiling after CBX2 knockdown in MDA-MB-468 cells.....	57
Figure 3.4 Knockdown of CBX2 causes upregulation of RBL2 and has no effect on E2F4 expression in MDA-MB-231 cells.....	59
Figure 3.5 Knockdown of CBX2 causes upregulation of RBL2 and has no effect on E2F4 expression in MDA-MB-468 cells.....	60
Figure 3.6 Gene expression profiling after CBX2 knockdown affects RBL2 target genes in MDA-MB-468 cells.....	62
Figure 3.7 RBL2 and E2F4 IP on MDA-MB-468 cells after knockdown of CBX2.....	64
Figure 3.8 Relative fold enrichment of RBL2 at RBL2 promoter sites in MDA-MB-231 cells.....	66
Figure 3.9 Relative fold enrichment of RBL2 at RBL2 promoter sites in MDA-MB-468 cells.....	68
Figure 3.10 CUT & RUN on MDA-MB-231 cells.....	70
Figure 4.1 Effect of CBX2 suppressing RBL2.....	79

## List of Tables

Table 2.1 RNA sequences for siRNA directed towards the coding sequence (CDS) region used in transfections.....	31
Table 2.2 Composition of 100ml of RIPA Buffer .....	33
Table 2.3 Composition of BSA standards.....	34
Table 2.4 Composition of 10% Resolving Gel and 4% Stacking Gel .....	35
Table 2.5 Composition of 5X Running Buffer .....	35
Table 2.6 Composition of 1X Transfer Buffer.....	36
Table 2.7 Composition of 1X TBST .....	37
Table 2.8 Composition of 1X TBS .....	37
Table 2.9 Composition of 10X TBS pH 7.6 .....	37
Table 2.10 Antibodies used for Western Blot Analysis.....	38
Table 2.11 Primer sequences. Working concentration of primers used in qPCR was 0.05µg/µl .....	41
Table 2.12 Composition of 5ml of Lysis Buffer.....	43
Table 2.13 Antibodies used for Co-IP .....	44
Table 2.14 Composition of 10ml of 11% Formaldehyde solution.....	45
Table 2.15 Composition of 100ml of Lysis Buffers 1/2/3 .....	46
Table 2.16 Antibodies used for ChIP.....	47
Table 2.17 Composition of 50ml of Elution Buffer.....	47
Table 2.18 Composition of 50ml of TE Buffer.....	48
Table 2.19 Antibodies used for CUT & RUN .....	50
Table 3.1 Data quality summary of CUT & RUN sequencing. “Sample” indicates what the target protein was and which antibody was used (Abcam or Diagenode for CBX2) as well as which biological repeat this DNA was from (n=1 or n=2). The sequencing was done in two batches. Which sample was in which batch is indicated by the red and blue shading .....	70

## Abbreviation List

ATCC – American type culture collection

BCA – Bicinchoninic acid

BD – Bromodomain

BET – Bromodomain and extraterminal domain

BL – Basal-like

BRCA – Breast cancer gene

BSA – Bovine serum albumin

CBX – Chromobox

cDNA – Complementary DNA

CDS – coding sequence

ChIP – Chromatin immunoprecipitation

CIN – Chromosomal instability

Co-IP – Co-Immunoprecipitation

COSHH – Control of substances hazardous to health

CUT & RUN – Cleavage under targets & release using nuclease

DMEM – Dulbecco's modified eagle medium

DP – Dimerisation partner

DSB – Double strand break

EED – Embryonic ectoderm development

ER – Oestrogen receptor

ERE – Oestrogen response element

EZH2 – Enhancer of zeste homolog 2

FBS – Foetal bovine serum

GBM – Glioblastoma multiforme

HAT – Histone acetyltransferase

HDAC – Histone deacetylase

HDM – Histone demethyltransferase

HER2 – Human epidermal growth factor receptor 2

HMT – Histone methyltransferase

HPH – Human polyhomeotic homolog

HR – Homologous recombination

IM – Immunomodulatory

K - Lysine

LAR – Luminal androgen receptor

LB – Lysis buffer

MES – Mesenchymal

MT - Methyltransferase

mTOR – Mammalian target of rapamycin

NAD<sup>+</sup> - Nicotinamide adenine dinucleotide

NHEJ – Non-homologous end joining

PARP – Poly (ADP ribose) polymerase

PBS – Phosphate buffered saline

PcG – Polycomb group

PCGF – Polycomb group factor

PDL1 – Programmed cell death ligand 1

PDX – Patient derived xenograft

PIC – Protease inhibitor cocktail

PIP<sub>2</sub> – Phosphatidylinositol 4,5-bisphosphate

PIP<sub>3</sub> – Phosphatidylinositol 3,4,4-triphosphate

PI3K – Phosphatidylinositol-3-kinase

PR – Progesterone receptor

PRAS40 – Proline rich Akt substrate 40

PRC – Polycomb repressive complex

P/S – Penicillin and streptomycin

PTEN – Phosphatase and tensin deleted on chromosome ten

PTEF-b – Positive transcription elongation factor

PTM – Post-translational modification

qPCR – Quantitative polymerase chain reaction

Rb – Retinoblastoma

RbAp 46/48 – Retinoblastoma suppressor associated protein 46/48

RBL2 – Retinoblastoma-like protein 2

RPMI 1640 – Roswell park memorial institute medium 1640

RT – Reverse transcription

SDS – Sodium Dodecyl Sulphate

SA-β-Gal – Senescence associated β-galactosidase

SERM – Selective oestrogen receptor modulator

shRNA – Short hairpin RNA

siRNA – Small interfering RNA

SIRT1 – Sirtuin 1

SRB – Sulforhodamine B

SSB – Single strand break

SUZ12 – Suppressor of zeste 12

TCGA – The cancer genome atlas

TNBC – Triple negative breast cancer

TSC – Tuberous sclerosis

TSG – Tumour suppressor gene

WR – Working reagent

YAP – Yes-associated protein

# Chapter 1 Background

## 1.1 Cancer

Cancer is a genetic disease caused by uncontrolled cell growth and formation of tumours which may then invade different areas of the body (metastasis). Tumours can either be benign, meaning they are not cancerous, or malignant (National Cancer Institute, 2021). There are over 200 different types of cancer and 1 in 2 people will develop cancer in their life (Cancer Research UK, 2022). In the UK the most common cancers are breast cancer, bowel cancer, prostate cancer, and lung cancer (Figure 1.1) (Cancer Research UK, 2022).

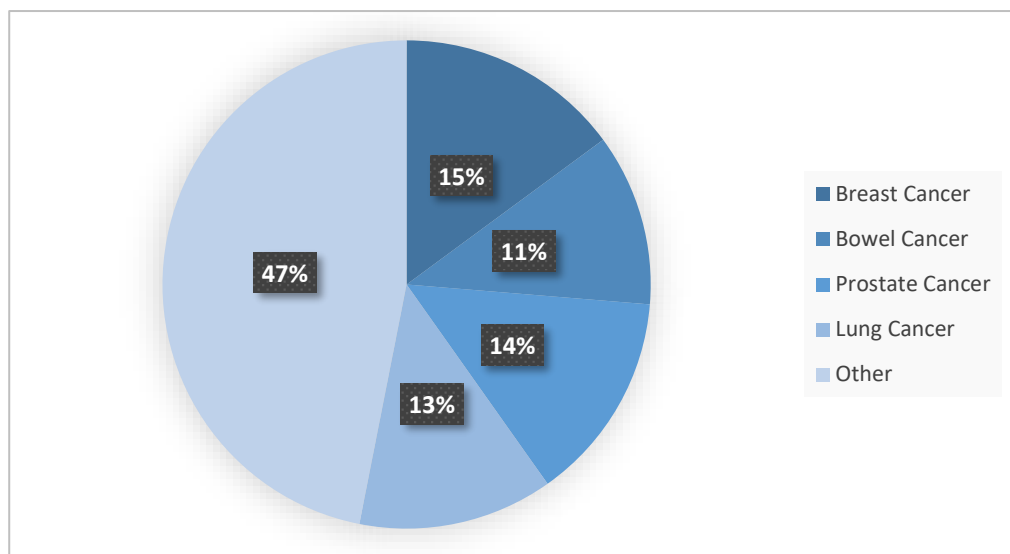


*Figure 1.1 Percentage of the 4 most common cancers vs other cancers*

Data taken from Cancer Research UK of the 4 most common cancers vs other cancers for 2016-2018. There are on average 55,920 breast cancer cases reported each year out of a total of 375,400 cancer cases (Cancer Research UK, 2022).

The risk factors that can lead to cancer can be categorised into different groups. The first group is intrinsic risk factors, such as DNA mutations caused by random and spontaneous errors in replication of DNA. There are also non-intrinsic risk factors such as radiation exposure, carcinogen exposure, and an individual's lifestyle, such as diet and smoking, which can affect cancer risk by inducing additional genetic mutations (Wu et al, 2018).

Hanahan and Weinberg proposed six hallmarks that contribute to the multi-step process of tumour initiation and progression. These hallmarks are sustaining proliferative signalling, evading growth suppressors, activating invasion and metastasis, enabling replicative

mortality, inducing angiogenesis and resisting cell death. Later it was proposed that these hallmarks are enabled by genomic instability and mutation (Hanahan & Weinberg, 2011). Genomic instability refers to the acquisition of alterations to the genome during cell division. One of the most common forms is chromosomal instability (CIN) which is when a cell has an abnormal number of chromosomes, a key factor contributing to cancer progression. CIN can lead to gain or loss of function mutations (Bielski & Taylor, 2021). Gain or loss of function mutations are associated with proto-oncogenes and tumour suppressor genes (TSGs). Proto-oncogenes play a key role in cell growth and when they undergo a gain of function mutation to become an oncogene, they contribute to cell transformation. TSGs work to prevent the formation of cancer through DNA damage repair, inhibition of cell division and inducing apoptosis of cells which incur genetic mutation. A loss of function mutation in TSGs stops them from preventing cells from proliferating when mutated, thus allowing the progression of cancer formation (Wang et al, 2019).

## 1.2 Breast Cancer

Breast cancer is a complex disease caused by the uncontrolled growth of mammary epithelial cells. Most commonly it develops within the cells that line the milk ducts in the breast tissue (Cancer Research UK, 2021). Between 2015 and 2017 in the UK there were 55,176 new breast cancer cases and between 2016 and 2018 there were 11,547 deaths due to breast cancer (Cancer Research UK, 2021). The main treatment options for breast cancer are surgery, radiotherapy and chemotherapy. One form of surgery option is to have a mastectomy which involves the removal of the breast which reduces the risk of the cancer developing. However, this can have other long-lasting psychological effects on the patient such as the risk of developing depression (Akram et al, 2017).

Using gene expression profiling and immunohistochemistry, breast cancer has been classified into four broad subtypes: oestrogen receptor (ER)+/luminal-like, basal like, human epidermal growth factor receptor-2 (HER2)+ and normal-like (Botstein et al, 2000). Further stratification has identified that the luminal subtype can be divided into two subtypes called luminal A and luminal B. Now breast cancer is classified into 5 molecular subtypes based, partly, through the presence and lack of hormone receptors and the proliferation marker, KI-67, as well as gene expression profiles (Sørliie et al., 2001). The hormone receptors used to identify the subtypes are the oestrogen receptor (ER), progesterone receptor (PR) and human

epidermal growth factor receptor-2 (HER2). The subtypes are luminal A (ER+, PR+, HER2-, KI-67-), luminal B (ER+, PR+, HER2-, KI-67+/ER+, PR+, HER2+, KI-67+), HER2 overexpression (ER-, PR-, HER2+), basal (ER-, PR-, HER2-, basal marker+) and normal-like (ER+, PR+, HER2-, KI-67-) (Dai et al, 2015). Normal-like and luminal A have similar molecular characteristics however studies have suggested that the normal-like subtype is due to high amounts of normal cells in the breast cancer tumour (Liu et al, 2014). Furthermore, Curtis et al, 2012 analysed over 2000 breast cancer tumours from the UK and Canada. The analysis was carried out to investigate whether there are more biological subgroups of breast cancer by using joint clustering of copy number and gene expression data. From the analysis it was discovered that there are 10 integrated clusters of subgroups which are grouped based on copy number aberrations. This discovery allows the intrinsic breast cancer subtypes to be further divided (Curtis et al, 2012).

The ER is present in Luminal A, Luminal B and normal-like breast cancer. Luminal A is the most common subtype, accounting for 50-60% of breast cancers. Patients with this type of breast cancer generally have a good prognosis. The Luminal B subtype is responsible for 15-20% of breast cancer. However, Luminal B tends to have a poorer prognosis and a lower survival rate. Luminal A and B are positive for ER and PR, but Luminal A is negative for HER2 receptor. Some Luminal B cancers are positive for HER2 receptor (Yersal & Barutca, 2014). The ER plays an important role in breast development. It works by the ligand oestrogen, or its metabolites, binding to the oestrogen receptor in the nucleus. This binding triggers the receptor to dimerise to form an ER homodimer. After dimerisation the ER binds to oestrogen response elements (EREs) which are located on the promoters of specific target genes and enhancer regions which drives expression of proliferative genes (Bjoernstoem & Sjoeborg, 2005). The ER has therefore been targeted by endocrine therapy to treat breast cancer. The main treatment is the use of selective ER modulators (SERMs) such as Tamoxifen. Tamoxifen works by mimicking oestrogen, thus being able to bind to the ER and acting as a competitive antagonist, preventing ER signalling and ultimately stopping cell proliferation. However, in many cases patients have become resistant to Tamoxifen which led to the development of other drugs that work by degrading the ER itself such as Fulvestrant (Carroll, 2016).

The HER2 positive subtype is responsible for 20% of breast cancers. This subtype is associated with a higher recurrence and mortality rate. HER2 is a tyrosine kinase receptor which is part of a superfamily of three other receptors called HER1, HER3 and HER4 (Patel

et al, 2020). HER2 in normal health is expressed by breast epithelial cells at low levels and plays a role in cell growth. In many breast cancers HER2 is overexpressed which leads to abnormal cell proliferation. HER2 is therefore also a therapeutic target and the drug Trastuzumab was developed to inhibit its activity (Vu & Claret, 2012). Trastuzumab has been found to work in different ways such as selectively blocking ligand-dependent HER2-HER3 dimerisation. This binding leads to the downregulation of the oncogenic P13K pathway and downstream mediators that allow cell cycle progression to continue, thus preventing cancerous cells to proliferate (Garjria & Chandarlapaty, 2011).

### 1.2.1 Triple negative breast cancer

Triple negative breast cancer (TNBC) shows no expression of ER, PR and HER2 and is responsible for 10-15% of all breast cancers (da Silva et al, 2020). Due to the lack of receptors, TNBC does not respond to endocrine therapy and the treatment options tend to be chemotherapy or surgery. The characteristics of TNBC are that it is an aggressive form of breast cancer with an early relapse rate and poor overall prognosis (da Silva et al, 2020). It has also been found to be common in women with a mutated breast cancer 1 or 2 gene (BRCA1/2). There are 6 subtypes of TNBC: basal-like 1 and 2 (BL1 and BL2), mesenchymal (MES), MES stem-like, immunomodulatory (IM) and luminal androgen receptor (LAR) (Lehmann et al, 2011).

Despite the lack of targeted therapeutics there are some new emerging treatments for TNBC, one being the use of Poly (ADP-ribose) polymerase (PARP) inhibitors. PARP is part of a family of enzymes that play a role in DNA repair, specifically, base excision repair for single strand breaks (SSBs). PARP1 recognises the damaged DNA site and binds to it along with nicotinamide adenine dinucleotide (NAD<sup>+</sup>). Once NAD<sup>+</sup> is bound, PARylation occurs where components of ADP-ribose from NAD<sup>+</sup> transfer to target proteins which allows the recruitment of repair factors to the damaged DNA. PARP1 then autoPARylates, releasing from the site so the DNA can be repaired (Chen, 2011; Cortesi et al, 2021). If these SSBs are not successfully repaired, it can lead to the formation of double strand breaks (DSBs) which is another form of DNA damage repaired by homologous recombination (HR). HR relies on the use of functional BRCA1/2 proteins. BRCA1 detects and binds to the DSBs and organises repair proteins at the damaged site and BRCA2 allows RAD51, a recombinase, to bind to the DNA repair site. If DSBs are not repaired it can lead to apoptosis (Chen, 2011). PARP

inhibitors work by preventing the autoPARylation of PARP1, thus it is trapped at the damaged DNA site and the SSBs cannot be repaired. This leads to the formation of DSBs and in patients with mutated BRCA1/2 genes, HR repair cannot be carried out. Therefore, another form of DNA repair for DSBs is carried out called non-homologous end joining (NHEJ), which is error prone and leads to accumulation of mutations and cell death (Mateo et al, 2019). There are two PARP inhibitors approved for the treatment of BRCA associated TNBC called olaparib and talazoparib. The OlympiAD and EMBRACA clinical trials, showed that both inhibitors caused a significant improvement in progression-free survival and health related quality of life compared to non-platinum single-agent chemotherapy (Tung & Garber, 2022). Treatment with Olaparib requires a 300 mg dosage twice a day whereas talazoparib requires a 1 mg dosage once a day. It has been found that talazoparib is 100-fold more potent and shows increased cytotoxicity compared to the effects of Olaparib (Min & Im, 2020). PARP inhibitors have been shown to be effective against breast cancer with mutated BRCA1/2 genes. The inhibitor and HR deficiency together results in synthetic lethality where the loss of two genes can lead to cell death through cell cytotoxicity, replication fork collapse and unrepaired DNA damage (Keung et al, 2019; Rose et al, 2020).

Another new treatment is the use of Programmed Cell Death Ligand 1 (PDL1) inhibitors (Chen et al, 2021). PDL1 is an immune checkpoint inhibitor that has an important role in inflammation regulation and maintaining T lymphocyte tolerance. PDL1 is often found expressed on the surface of dendritic cells, B cells, T cells, monocytes and natural killer T cells. The pathway works through the binding of PD-1 to PDL1/2 which then activates the inhibition of the T cell response, reduced cytokine production and tolerance to antigens (Schütz et al., 2017). It has been found that some TNBC tumours can also express PDL1 on their surface as an 'immune escape'. This expression of PDL1 inactivates the T cell response which prevents the tumour from being recognised by immune checkpoints and the immune system. PDL1 inhibitors act by stopping this effect and activating the immune response to target the tumour cells (Erber & Hartmann, 2020). A PDL1 inhibitor was approved in 2020 called pembrolizumab (Keytruda). It was found in the KEYNOTE-355 trial that using this inhibitor alongside chemotherapy showed a better progression-free survival than just chemotherapy alone in metastatic TNBC (Cescon et al, 2020).

Despite a few new and upcoming treatments for TNBC, the prognosis of this subtype remains poor and new therapeutic options are needed.

## 1.3 Epigenetics

### 1.3.1 Chromatin

DNA is packaged into chromatin which is composed of nucleosomes. A nucleosome consists of 147bp of DNA wrapped around an octamer of histone proteins; 2 copies each of histone H2A, H2B, H3 and H4 (Figure 1.2). The histones also have protruding amino acid tails that can undergo post-translational modification (PTM) (Audia & Campbell, 2016).

Chromatin can be organised into heterochromatin and euchromatin. In areas of the genome where heterochromatin is found there is little/no transcription due to the nucleosomes being tightly condensed which means genes cannot be accessed by RNA Polymerase II and there is no gene expression. In areas of euchromatin, the DNA is loosely packaged allowing for transcription by RNA Polymerase II and the potential for gene expression. PTM of the histone tails can influence this chromatin state (Bannister & Kouzarides, 2011).

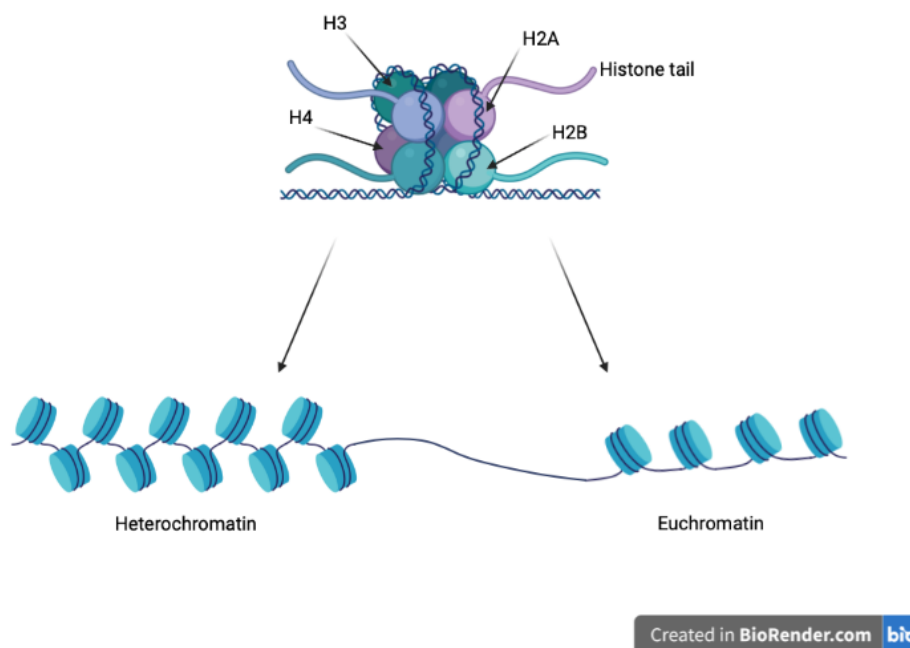


*Figure 1.2 Chromatin Structure*

Chromatin structure showing the histone proteins and amino acid tails forming the nucleosome structure and how it is arranged to form heterochromatin or euchromatin. The nucleosome at the top of the figure can also be seen in figure 1.3.

### 1.3.2 Histone post-translational modifications (PTMs)

The histone amino acid tails are rich in lysine and arginine residues that can undergo PTMs and alter the chromatin state. PTMs can change the compaction of nucleosomes which leads

to either the formation of euchromatin or heterochromatin thus affecting transcription and gene expression (Audia & Campbell, 2016). There are different PTMs that can occur such as acetylation, methylation and phosphorylation (Bannister & Kouzarides, 2011). There are a number of chromatin modifying proteins that play a role in the addition, removal and recognition of PTMs known as writer, eraser and reader proteins. Writer enzymes modify the amino acid tails by adding PTMs. Erasers work by removing the PTMs put in place by writers and readers recognise specific PTMs (Biswas & Rao, 2018).

Histone acetylation is a form of histone modification which works by the addition of acetyl groups from acetyl-CoA onto lysine residues. The addition of an acetyl group is carried out by writer proteins called histone acetyltransferases (HATs). Acetyl groups have a negative charge therefore when they are added by HATs to the amino acid tails this neutralises the positive charge of histones. This then leads to the weakening of the electromagnetic attraction between negatively charged DNA and the histone proteins, therefore loosening chromatin structure and allowing the formation of euchromatin. This modification can be reversed by eraser proteins called histone deacetylases (HDACs) that remove the acetyl group. When deacetylation occurs, this condenses the chromatin into heterochromatin and transcription cannot occur (Guo et al, 2018).

Another type of histone modification is methylation. Methyltransferases (MTs) are enzymes that add methyl groups to various substrates in different important biological processes (Abdelraheem et al., 2022). Histone methyltransferases (HMTs) add a methyl group onto the lysine and arginine residues of the histone amino acid tails. Lysine can be mono- (me1), di- (me2) or tri- (me3) methylated and arginine can be mono- or di-methylated. This can be reversed by histone demethylases (HDMs) (Fallah et al, 2021; Zhuang et al, 2020). It has been found that after the addition of a methyl group, reader proteins containing either the chromodomain, tudor domain or WD-40-repeat domain can recognise the PTM and recruit molecules which then go on to alter the chromatin and transcriptional state. The outcome of whether chromatin will be transcriptionally repressed or active depends on the location and degree of the methylation (Greer & Yang, 2012; Zhang & Martin, 2005). For example, the methylation of lysine (K) on H3 (H3K4) is known to be associated with transcriptional activation whereas the methylation of H3K9 is associated with transcriptional repression (Hyun et al, 2017).

Phosphorylation is the addition of a phosphate group which is regulated by kinases and phosphatases. This can occur on all four of the histone tails specifically on the tyrosine, serine and threonine residues. This process can be reversed. Phosphorylation is associated with transcription and gene expression as the bonds between the DNA and histones are weakened thus loosening the chromatin structure forming euchromatin (Shanmugan et al, 2018).

### 1.3.3 Dysregulation of histone modifications and cancer

Dysregulated epigenetic modification of histone proteins and the subsequent alteration of gene expression patterns to drive cancer growth have been found to play an important role in various types of cancer, such as gastric, prostate and lung cancer, which has helped with the prediction of clinical outcomes (Elsheikh et al, 2009). Altered activity and expression of epigenetic regulatory proteins have also been found to play key roles in cancer development. For example, it has been found that some HDACs and HMTs are upregulated in breast, colon and prostate cancer (Kanwal & Gupta, 2012). An example of an epigenetic protein involved in some cancers is sirtuin 1 (SIRT1). SIRT1 is a HDAC that was recently discovered to target H4K4ac in breast cancer and the HDAC is also responsible for the removal of acetylation from H1K26, H3K9 and H4K16. SIRT1 plays an important role in the DNA damage response by both acting as HDAC at DNA damage sites and as a HDAC that specifically targets crucial proteins required for DNA repair. SIRT1 has been studied in different cancers showing a difference in expression, for example the overexpression of SIRT1 was identified in colon, prostate, leukaemia, non-melanoma and melanoma skin cancer. On the other hand, it was found to be down regulated in hepatic cell and breast cancer (Alves-Fernandes & Jasiulionis, 2019).

Considering the oncogenic role of dysregulated epigenetic signalling and, or, specific epigenetic regulators, targeting epigenetic proteins may be a novel way to treat cancer.

### 1.4 Polycomb Repressive Complex 1 (PRC1)

The PRC1 complex is an enzymatic multiprotein complex consisting of Polycomb Group (PcG) proteins. PcGs can form PRC1 and PRC2. PcG proteins are a family of proteins known to regulate gene expression through epigenetically repressing the transcription of genes (Chittock et al, 2017). PRC1 does this by modulating chromatin structure. PRC1 is formed by four different proteins. These proteins are Chromobox (CBX), Polycomb Group Factor

(PCGF), Human Polyhomeotic Homolog (HPH) and the E3 ligase protein (RING). However, there are multiple versions of the PRC1 complex as there are different orthologues of the protein subunits (Gil & O’Loughlen, 2014). There are 5 forms of CBX (2,4,6,7,8), six forms of PCGF (1,2,3,4,5,6), three forms of HPH (1,2,3) and two RING proteins (1 and 2). PRC1 can be canonical, which includes a CBX protein in its composition or non-canonical where there is no CBX protein (Geng & Gao, 2020). The components of PRC2 are enhancer of zeste homolog 2 (EZH2), embryonic ectoderm development (EED), suppressor of zeste 12 (SUZ12) and retinoblastoma suppressor associated protein 46/48 (RbAp46/48) (Shi et al, 2017). PRC2 tri-methylates K27 on H3 (H3K27me3) (Gahan et al, 2020). A chromodomain in CBX proteins recognises this modification and binds to it (Figure 1.3). The RING protein within the associated PRC1 complex ubiquitinates K119 on H2A (H2AK119ub) (Figure 1.3). This results in the chromatin becoming condensed to form heterochromatin (Gil & O’Loughlen, 2014).

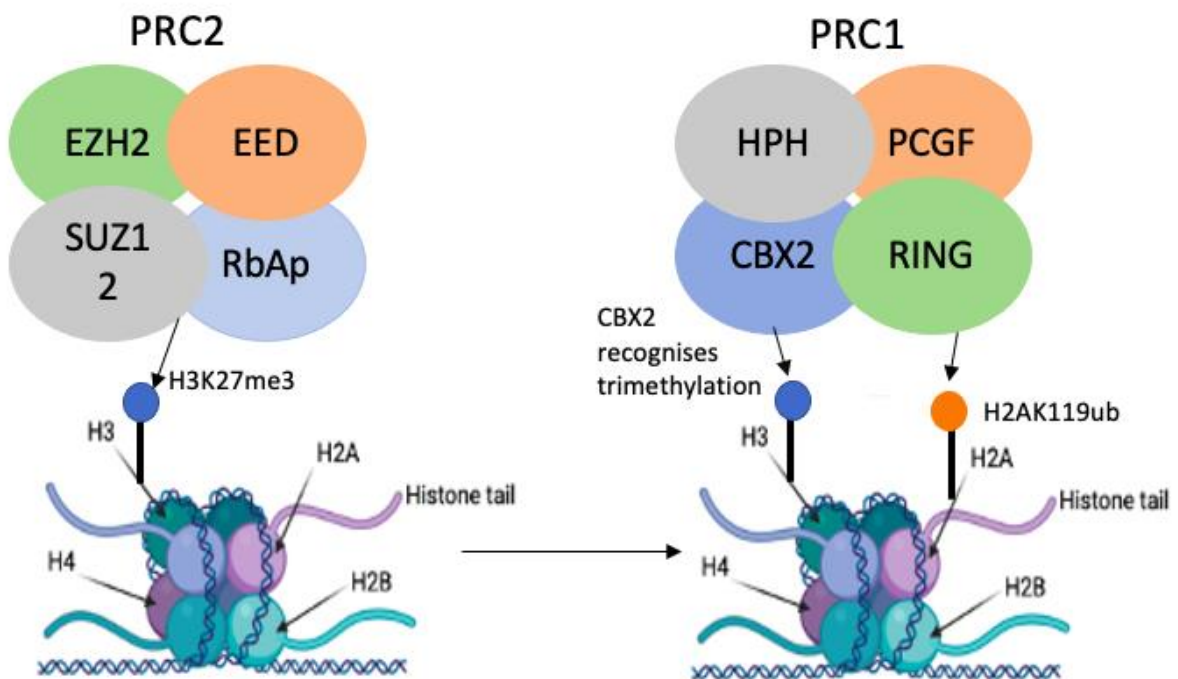


*Figure 1.3 PRC1 and PRC2*

PRC2 trimethylates H3K27 which is recognised by the CBX protein in PRC1 (CBX2 in the example above). The RING protein in PRC1 ubiquitinates H2AK119 leading to the condensing of chromatin and transcriptional repression.

## 1.5 CBX2

CBX2 has an N terminal and adjacent to this there is an AT hook DNA binding domain. When the chromodomain in CBX2 recognises specific PTMs e.g., H3K27me3, the AT hook can bind to the groove in an AT rich region on the DNA site next to the chromodomain and trap it in place until CBX2 is released (Senthilkumar & Mishra, 2009). In addition to this, CBX2 also has a carboxyl (c) terminal polycomb repressor box which interacts with RING1 proteins thus signalling the RING protein in PRC1 to ubiquitinate K119 on H2A (Kawaguchi et al, 2017).

### 1.5.1 CBX2 and cancer

In 2014, Clermont et al carried out a systematic meta-analysis of one of the PRC1 components, CBX2. Within this analysis there was a genomic analysis of the *CBX2* locus. This involved using the COSMIC database to analyse *CBX2* mutations. It was discovered that there was a low frequency of alterations within CBX2 in cancer, suggesting that a functioning version of CBX2 was important for cancer development. Data from the OncoPrint database was used to carry out a transcriptomic analysis of human cancers including colon, breast, stomach, and lung cancer. The analysis showed that in all the cancers analysed there was an upregulation of *CBX2* and no downregulation of *CBX2* (Clermont et al, 2014). As well as this, the OncoPrint analysis showed that 9 studies reported high *CBX2* mRNA levels in metastatic tumours compared to primary tumours (Clermont et al, 2014). In addition, a study that used data from The Cancer Genome Atlas (TCGA) identified that *CBX2* is highly expressed in hepatocellular cancer and this overexpression is associated with poor prognosis. Experiments were carried out knocking down CBX2 expression in hepatocellular cancer cell lines which decreased proliferation across the cell lines (Mao et al, 2019). RNA sequencing data from this study identified that CBX2 may regulate the Hippo pathway which regulates cell proliferation and apoptosis. This pathway is regulated by the Yes-Associated Protein (YAP). YAP can be inactivated by phosphorylation; however, the protein Wt1-interacting protein (WTIP) can prevent this phosphorylation. RNA sequencing showed *WTIP* being one of the significant differential genes identified. Thus, it is believed that after CBX2 knockdown, *WTIP* is inhibited which leads to the phosphorylation of YAP which in turn leads to decreased proliferation and increased apoptosis in hepatocellular cancer cell lines (Mao et al, 2019). Another study carried out a gene expression microarray analysis on RNA from the metastatic LTL313H and non-metastatic LTL31B patient derived xenograft (PDX) prostate cancer models. This analysis showed that *CBX2* was upregulated in the LTL313H

model which was also confirmed with quantitative PCR (qPCR) analysis, suggesting that CBX2 promotes tumour metastasis. To further investigate the link of CBX2 and prostate cancer, MANOVA analysis showed that overexpression of *CBX2* was associated with a lower patient age, higher Gleason grade and a positive nodal status which contributes to poor clinical outcome in patients (Clermont et al, 2016). Due to studies finding CBX2 to be overexpressed in a range of different cancers this suggests that CBX2 could be a potential therapeutic target.

### 1.5.1 CBX2 and breast cancer

Studies have found CBX2 expression to be upregulated in breast cancer. An analysis of the Cancer Cell Line Encyclopedia (CCLE) database showed that out of all cancers analysed breast cancer was the 5<sup>th</sup> highest for *CBX2* expression (Liang et al, 2017). Oncomine analysis showed that CBX2 was expressed 9.378-fold higher in breast cancer samples compared to normal samples, and an Xena Public Data Hubs analysis showed that CBX2 expression is strongly linked to TNBC compared to other subtypes of breast cancer (Liang et al, 2017). Iqbal et al, (2021) also found a link between CBX2 and breast tumour cell proliferation. Experiments were carried out using a TNBC cell line MDA-MB-231 and an ER+ breast cancer cell line MCF-7 and siRNAs targeting CBX2 were used to knockdown CBX2 in these cell lines. After knockdown, it was observed that there was a decrease in cell number in CBX2 depleted cells compared to the control cells in both cell lines, suggesting a role for CBX2 in breast cancer cell growth (Iqbal et al, 2021).

It has also been found that CBX2 may play a role in altering the phosphatidylinositol-3-kinase (PI3K)/AKT/mammalian target of rapamycin (mTOR) signalling pathway in breast cancer (Zheng et al, 2019). The PI3K/AKT/mTOR pathway plays a key role in regulation of cell growth, motility, survival, metabolism and angiogenesis. PI3K is a lipid kinase with 3 subunits called: p85 regulatory subunit, p55 regulatory subunit and p110 catalytic subunit. There are different versions of PI3K called Class 1A, Class 1B, Class 2 and Class 3 and it is Class 1A that have been studied the most and been found to be involved with the progression of cancer (Yang et al, 2019). PI3K is an important component of the pathway. Phosphatidylinositol 4,5 biphosphate (PIP<sub>2</sub>) is phosphorylated by PI3K to become phosphatidylinositol 3,4,4-triphosphate (PIP<sub>3</sub>) which then leads to the phosphorylation of AKT. This ultimately influences the cancer cell cycle, survival and growth.

Dephosphorylation of PIP3 to PIP2, is carried out by the TSG phosphatase and tensin homolog deleted on chromosome ten (PTEN). Downstream of this PI3K/AKT is mTOR which consists of Raptor, mLST8 and proline rich Akt substrate 40 (PRAS40); there are two different mTOR complexes, mTORC1/2. mTORC1 when stimulated plays a role in cell metabolism and anabolic cell growth. This happens when Akt activates mTORC1 phosphorylating and inhibiting tuberous sclerosis 1 or 2 (TSC1/2) which then phosphorylates PRAS40 (Paplomata & O'Regan, 2014). Through gene set enrichment analysis of the cancer genome atlas (TCGA) dataset of 1079 breast cancer tumour samples and 104 non-tumour breast tissue samples, there was a positive correlation between *CBX2* expression and activation of the PI3K/AKT/mTOR pathway (Zheng et al, 2019). Further experiments showed the downregulation of *PI3KCA*, *PIK3CD* and *mTOR* genes after gene silencing of *CBX2*, thus it has been proposed that the PI3K/AKT/mTOR pathway works downstream of *CBX2* and that *CBX2* plays a role in regulating the pathway (Zheng et al, 2019). This pathway has also been found to be activated in glioblastoma multiforme (GBM) and these patients tend to have a poorer prognosis. The molecular level of this pathway was further investigated in GBM patients and genetic alterations were seen. For example, loss of PTEN expression was observed which has a key part in the pathway as it can reverse the process (Li et al, 2016).

Overall, there appears to be a link between *CBX2* function and breast cancer, particularly in TNBC, suggesting it may be a therapeutic target in this hard-to-treat cancer.

## 1.6 RBL2 and E2F4

A previous study by Bilton et al, 2022 has shown that knockdown of *CBX2* expression reduces breast cancer cell line growth, which agrees with previous findings. RNA-sequencing analysis of *CBX2* depleted cells showed downregulation of proliferative genes and reduced expression of *E2F* target genes. In addition, *CBX2* knockdown reduced the expression of genes known to be regulated by the tumour suppressor gene *RBL2*. *RBL2* gene expression also increased following *CBX2* knockdown.

Regulation of the cell cycle is critical in preventing cancerous cells from proliferating. It is known that a key factor of cancer progression in many cancers is dysregulation of the cell cycle (Sadasivam & DeCaprio, 2013). An important regulator of the cell cycle is the E2F family of transcription factors. There are 8 proteins within this family that can be separated

into categories depending on their role. E2F1/2/3A are classed as transcriptional activators and they are expressed at the G1 phase until the S phase. E2F7/8 are transcriptional atypical repressors that are expressed in the late S phase and then E2F3B/4/5/6 are transcriptional canonical repressors that are expressed throughout the whole of the cell cycle (Kent & Leone, 2019). E2F regulates the cell cycle by interacting with the retinoblastoma (Rb) gene family. The Rb family consists of retinoblastoma-like protein 2 (RBL2)/ p130, Rb/p105 and RBL1/p107 which are TSGs (Litovchick et al, 2007). Rb/RBL1/RBL2 and E2F4 interact to form a multi-subunit protein complex along with dimerization partner (DP) and MuvB to form the DREAM complex (Sadasivam & DeCaprio, 2013). Once the DREAM complex is bound to DNA the RBL2 component of the DREAM complex recruits chromatin modifying enzymes to the promoters on E2F4 target genes which leads to transcriptional repression of cell cycle regulatory genes bringing the cell cycle to a halt (Litovchick et al, 2007). The inhibition of the DREAM complex can cause cancerous cells to move from G1 phase to S phase therefore instigating cell replication (Sadasivam & DeCaprio, 2013). It is therefore hypothesised that CBX2 may repress *RBL2* expression, which then leads to inhibition of DREAM complex formation in breast cancer which in turn allows cancer growth.

## 1.7 Thesis Aims

### 1.7.1 Hypothesis

CBX2 promotes cell growth in TNBC via downregulation of *RBL2* and therefore inhibition of the DREAM complex.

### 1.7.2 Aims

1. Show successful knockdown of CBX2 in TNBC cell lines
2. Investigate the effect of CBX2 knockdown on cell growth in TNBC cell lines
3. Investigate the effect of CBX2 knockdown on *RBL2* and *E2F4* protein expression in TNBC cell lines
4. Investigate the effect of CBX2 knockdown on *RBL2* target gene expression in TNBC cell lines
5. Investigate the effect of CBX2 knockdown on *RBL2*/DREAM complex activity in TNBC cell lines
6. Identify areas of the genome CBX2 is bound to in TNBC cells

### 1.7.3 Ethical Considerations

The cell lines (MDA-MB-231 and MDA-MB-468) used in this study were purchased from American Type Culture Collection (ATCC). Throughout the project Control of Substances Hazardous to Health (COSHH) forms were read and completed before experiments that were carried out in the laboratory.

## Chapter 2. Materials and Methods

### 2.1 Cell Culture

All cell culture procedures were carried out in a Biosafety Cabinet Class II.

MDA-MB-468 cells and MDA-MB-231 cells were obtained from ATCC. MDA-MB-468 cells were cultured in Dulbecco's Modified Eagle Medium (DMEM) (Gibco, UK) containing 10% Foetal Bovine Serum (FBS) (Gibco, UK) and 1% Penicillin and Streptomycin (P/S) (Lonza, UK) MDA-MB-231 cells were cultured in Roswell Park Memorial Institute Medium (RPMI 1640) (Gibco, UK) containing 10% FBS and 1% P/S. Cells were maintained in a Nuair incubator at 37°C and 5% CO<sub>2</sub>. In routine cell culture media was changed every 3 days.

### 2.2 Trypsinisation

1X Phosphate Buffered Saline (PBS) was made using 200X concentrated PBS tablets in deionised water (Fisher Bioreagents, UK) and then autoclaved. A 1:30 dilution of Trypsin (Sigma, UK) was made up in 1X PBS and both were warmed to 37°C prior to use. The media was first removed from the flask and discarded. Flasks containing the cells were washed with 1X PBS and gently rocked to ensure the cell layer on the base of the flask was covered. The PBS was then removed and discarded. Trypsin was added so that it completely covered the cell monolayer and was then placed into an incubator at 37°C and 5% CO<sub>2</sub> for 2-5 minutes, depending on the cell line. After incubation the cells were checked under a microscope to ensure the cells had detached from the flask. Once detached, trypsin was neutralised using cell culture media (at least a 1:4 dilution of the trypsin with media). The cell suspension was then transferred to a 50 ml falcon tube and spun in a centrifuge (Eppendorf, Centrifuge 5702) for 3 minutes at 0.3 RCF. The media was then removed from the cell pellet and discarded. The cell pellet was resuspended in fresh media and the appropriate amount of cell suspension (depending on the number of cells required) was put into a new flask. Any remaining cell suspension was discarded. The flasks were placed into an incubator at 37°C and 5% CO<sub>2</sub>.

### 2.3 Counting cells

For experiments which required a precise number of cells to be used, the falcon tube containing the cells resuspended in media following trypsinisation was mixed and cell suspension was pipetted onto a haemocytometer chamber underneath a coverslip; ensuring the full chamber was covered. The number of cells in the top left, middle and bottom right squares on the haemocytometer were counted and used to calculate the cell number in 1 ml

(Figure 2.1). The average cell number ( $n$ ) from those squares on the haemocytometer is equivalent to  $n \times 10^4$  cells/ml, this number was then used to calculate different cell numbers needed for different experiments.

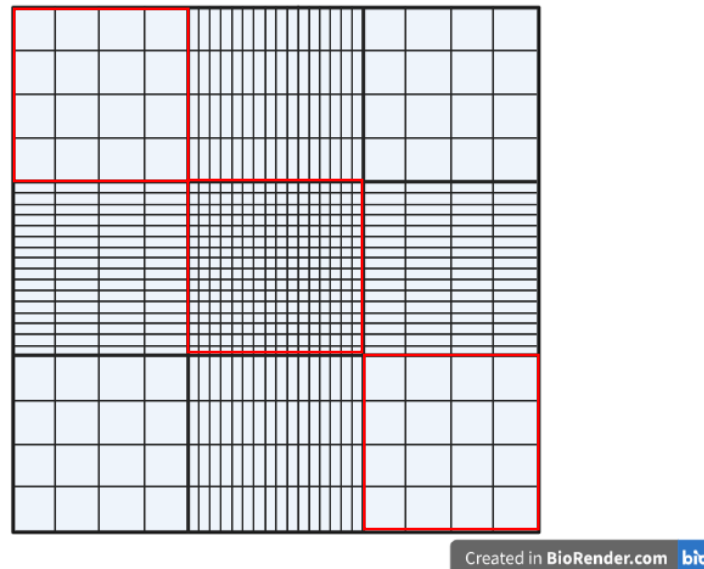


*Figure 2.1 Field on haemocytometer used to count cells*

3 counts were taken, one from the top left, one from the middle and then from the bottom right square (Highlighted with red outline). The counts were then averaged, and this gave  $n \times 10^4$  cells/ml.

#### 2.4 Cell Transfection

Small interfering RNAs (siRNA) that target CBX2 were used to knockdown CBX2 in the MDA-MB-468 cell line and MDA-MB-231 cell line. A control siRNA was also used called scrambled siRNA (siSCR). This is a non-silencing siRNA that has a sequence which does not correspond to any mRNA sequence in the human transcriptome. Three CBX2 targeting siRNAs were used (called number 1, 3 and 4) (Table 2.1). A master mix was prepared for each siRNA so that the final concentration of siRNA used in the transfection was 25 nM. For a transfection in a single well of a 6 well plate, in which 2 ml of cell suspension would be added, 100  $\mu$ l of basal media (Gibco, UK) (warmed to room temperature), 2  $\mu$ l of RNAiMAX (Thermofisher, UK) and 1  $\mu$ l of siRNA (50 $\mu$ M stock) (Table 2.1) were pipetted into a sterile autoclaved microcentrifuge tube to create a transfection master mix. This master mix can be scaled up and down depending on the total amount of media the transfection mixture will be added to.

The master mixes were pipetted up and down to ensure mixing and then left to incubate at room temperature for 20 minutes. During this time, the cell line being used was trypsinised and a cell count was carried out. 150,000 cells/well were used for a 6 well plate. The master mix was pipetted into the center of the well of a 6 well plate and 2 ml of the cell suspension was added with a stripette down the side of the well. The plate was gently rocked to ensure thorough mixing. The plate was then placed into an incubator at 37°C and 5% CO<sub>2</sub> for the duration of the experiment.

*Table 2.1 RNA sequences for siRNA directed towards the coding sequence (CDS) region used in transfections*

siRNA	RNA sequence	Company
siSCR	UUCUCCGAACGUGUCACGU	Sigma
SiCBX2 1	AGGAGGUGCAGAACCGGAA	Sigma
SiCBX2 3	GCAAGGGCAAGCUGGAGUA	Sigma
SiCBX2 4	CAAGGAAGCUCACUGCCAU	Sigma

## 2.5 Cell count assay

MDA-MB-468 cells were transfected with siSCR or siCBX2 #1/3/4 and grown for 96 hours in a 6 well plate in an incubator at 37°C and 5% CO<sub>2</sub>. After incubation, media from the wells was removed and the wells were washed with 1X PBS. The 1X PBS was discarded and the cells were trypsinised with 300 µl of trypsin and placed in an incubator at 37°C and 5%. Once the cells had detached 700 µl of media was added to the wells and then transferred to 1.5 ml microcentrifuge tubes. The cells were centrifuged for 3 minutes at 0.3 RCF. The media was removed from the cell pellet and the cell pellet was resuspended in fresh media. Cells were counted as seen above in section 2.3. The data was analysed in excel and for each experiment each siCBX2 condition was made relative to siSCR.

## 2.6 Sulforhodamine B (SRB) Assay

MDA-MB-468 cells were transfected with siSCR or siCBX2 #1/3/4 and grown in a 96 well plate in an incubator at 37°C and 5% CO<sub>2</sub>. Each condition had 5 wells of repeats with 10,000 cells per well in 200 µl of media and were grown for 96 hours. After incubation, 50% cold Trichloric acid in deionised water (v/v) (ThermoFisher Scientific, UK) was added to each well to a final % v/v of 10% and incubated at 4°C for 1 hour. After incubation, the plate was washed 4 times in water. The plate was tapped on blue roll to remove any excess water and left to air dry at room temperature. After drying, 50 µl of 0.4% SRB in 1% acetic acid (Alfa Aesar) was added to each well using a multi-well pipette and then incubated at room temperature for 1 hour. After incubation, the plate was washed 4 times in 1% acetic acid. The plate was tapped on blue roll to remove any excess acetic acid and then left to air dry at room temperature. 100 µl of 10 mM Tris buffer pH 10.5 was added to each well and placed on a shaker for 20 minutes. After shaking, the absorbance of the wells was read using the Gen5 software version 1.08 on The Synergy HT (BioTek) plate reader at 510nm. The data was analysed using excel and for each experiment each siCBX2 condition was made relative to siSCR.

## 2.7 Western Blot Analysis

### 2.7.1 Protein lysis

Media was removed from cells and discarded. For cells growing in 6 well plates, cells were washed with 1X PBS. The cells were either lysed with RIPA buffer (Table 2.2) or Sodium Dodecyl Sulphate (SDS) sample buffer (125mM Tris-HCl pH 6.8, 10% Glycerol, 2% (w/v) SDS). For SDS sample buffer lysis, the confluency of the cells was checked using a microscope and this affected the amount of SDS buffer added to each well. The cells were then scraped using a pipette and pipetted into microcentrifuge tubes and then stored at -20°C until further use. Cells that were lysed with RIPA were then rocked on ice for 30 minutes. After the incubation, the wells were scraped with cell scrapers and the lysate was pipetted into microcentrifuge tubes. The cells were then centrifuged at 16 x g for 3 minutes. The supernatant was pipetted into new microcentrifuge tubes and then stored at -20°C until further use.

Table 2.2 Composition of 100ml of RIPA Buffer

Reagent	Amount	Final Concentration
HEPES-KOH 0.5M pH 7.5	10ml	50 mM
LiCl 2M	25ml	0.5 M
EDTA 0.5M	200µl	1 mM
NP40	1ml	1%
Na-deoxycholate	0.7g	0.7%
Molecular Grade H <sub>2</sub> O	63.84ml	-

### 2.7.2 Bicinchoninic acid (BCA) assay

After proteins were lysed with RIPA buffer, a Pierce™ BCA Protein Assay Kit (Thermoscientific, UK) assay was used to quantify the protein in the samples. This was done by comparing the samples to a serial dilution of Bovine Serum Albumin (BSA) standards through colourimetric analysis using a plate reader. The serial dilutions were composed of BSA and RIPA buffer as the diluent (Table 2.3). Once this was done, the amount of working reagent (WR) required was calculated using the formula (# standards + # unknowns) x (# replicates) x (volume of WR per sample) = total volume of WR needed. This was then made up in a 50:1 dilution of Reagent A and Reagent B from the kit. The samples were diluted 1:8 with RIPA buffer. 25 µl of standards and samples were pipetted into a 96 well plate in triplicates. Then 200 µl of WR was added to each well and then placed on a plate shaker for 30 seconds. The plate was covered with foil to prevent exposure to light and incubated at 37°C and 5% CO<sub>2</sub> for 30 minutes. After incubation, the plate was read using the Gen5 software version 1.08 on The Synergy HT (BioTek) plate reader at 562nm. The data from the plate reader was used to plot a standard curve and the equation given from the curve was used to calculate the concentration of protein in the samples. This was done so equal amounts of

protein were loaded for Western blot analysis for each sample tested. The amount of SDS buffer added to the samples was 1:5 of the total volume of sample.

*Table 2.3 Composition of BSA standards*

Tube	Volume of Diluent (µl)	Volume of BSA (µl)	BSA Concentration (µl/ml)
A	-	700 of Stock	2000
B	400	400 of A	1000
C	450	300 of B	400
D	400	400 of C	200
E	400	100 of D	40
F	400	-	0

### 2.7.3 Gel Electrophoresis

A spacer plate (Biorad, UK) and a short plate (Biorad, UK) were put together in a frame and put onto a stand to create the mould for the gel. The mould was filled with deionised water for 5 minutes to ensure there was no leakage and then removed. A 10% acrylamide resolving gel (Table 2.4) was prepared in a 50 ml falcon tube and then pipetted into the gel mould on the stand and a layer of isopropanol was pipetted on top to ensure the gel set level, this was then left for the gel to polymerise. A 4% acrylamide stacking gel (Table 2.4) was prepared once the resolving gel had set in the gel mould. The isopropanol was removed from the top of the gel then the stacking gel was pipetted on top. 10 or 15 well forming combs were placed into the gel and left to polymerise. Whilst the gel polymerised, the lysates being used were boiled at 100°C for 10 minutes. After the gel polymerised, this was placed into a cassette and then into an electrophoresis tank, the comb was then removed. 1X running buffer in water (5X Running buffer -Table 2.5) was poured in the tank covering the gel. PageRuler pre-stained protein ladder (Thermofisher, UK) was loaded into the first well and then protein lysate was loaded into the rest of the wells. The tank was connected to a powerpack (Biorad, UK) via electrodes and the gel was run at 100 V for 1 hour and 30 minutes.

*Table 2.4 Composition of 10% Resolving Gel and 4% Stacking Gel*

Reagents	Amount for 10% resolving gel	Final concentration for resolving gel	Amount for 4% stacking gel	Final concentration for stacking gel
Distilled H <sub>2</sub> O	7.5ml	-	3.1ml	-
1.5M Tris Buffer 8.5 pH	3.7ml	368 mM	-	-
0.5M Tris Buffer 7.4 pH	-	-	1.25ml	127 mM
40% Acrylamide	3.6ml	10%	0.5ml	4%
10% SDS	150 µl	0.1%	50 µl	0.1%
10% APS	69 µl	0.05%	30 µl	0.06%
99% TEMED	46 µl	0.3%	10 µl	0.2%

*Table 2.5 Composition of 5X Running Buffer*

Reagents	Amount	Final Concentration
SDS	5g	17 mM
Tris	30g	248 mM
Glycine	144g	1.9 M
Distilled H <sub>2</sub> O	1000ml	-

#### 2.7.4 Protein Transfer

Following gel electrophoresis 1X transfer buffer (Table 2.6) was poured into a transfer tank. Next, a sponge was placed on a transfer cassette followed by 2 pieces of whatman paper (Cytiva, UK), the acrylamide gel, nitrocellulose blotting membrane (Cytiva, UK), 2 pieces of whatman paper and another sponge. This was closed and then placed inside the tank with the black side of the cassette facing to the negative electrode so the current will pass through the gel and transfer the proteins onto the membrane. Transfer buffer was poured into the tank so that the transfer cassette was submerged. This was put in ice and the transfer was run at 100 V for 1 hour.

Table 2.6 Composition of 1X Transfer Buffer

Reagents	Amount	Final Concentration
35 mM SDS	10g	3.5 mM
200 mM Tris	24.24g	20 mM
1.5M Glycine	111.75g	150 mM
Methanol	-	10 % v/v
Distilled H <sub>2</sub> O	up to 1000ml	-

### 2.7.5 Immunoblotting

Following transfer, 5% skimmed milk solution in 1X TBST (Table 2.7) was then poured onto the membrane taken from the transfer cassette and rocked for 1 hour to block the membrane from non-specific binding. After 1 hour the milk buffer was removed and the membrane was placed into a dilution of primary antibody (Table 2.10) in 5% skimmed milk solution in a falcon tube. This was put onto a roller in a cold room (4°C) overnight. After the incubation, the membrane was put onto a rocker and washed in 1X TBST 3 times for 10 minutes. The membranes were then placed into a dilution of secondary antibody (Table 2.10) in 5% skimmed milk solution in a falcon tube. The falcon tube was put onto a roller at room temperature for 1 hour. After the incubation, the membrane was washed again in 1X TBST 3 times for 10 minutes then the membrane was washed for 5 minutes in 1X TBS (Table 2.8). Using the Clarity Western ECL Substrate kit (Biorad, UK) enough ECL was prepared to cover each membrane in a 1:1:2 ratio of clarity substrate: peroxide + luminal/enhancer: 1X TBS. After this the membrane was taken to the ChemiDoc XRS+ imager (Biorad). The membrane was placed on the tray in the Chemi doc and the ECL was pipetted onto the membrane ensuring there were no air bubbles. ImageLab software was used to capture the image. The protein ladder was visualised first by selecting the colourimetric option from the blots tab. The mini protean gel type was selected. The membrane was positioned correctly on the tray and visualised. After the ladder was visualised the chemi option was selected from the blots tab. Mini protean gel type was used and the signal accumulation mode was selected. 50 images were taken between 1 second and 300 seconds. Whilst running, the clearest image was selected and saved.

*Table 2.7 Composition of 1X TBST*

Reagents	Amount	Final Concentration
Distilled H <sub>2</sub> O	900ml	-
10X TBS (200 mM Tris, 1.5M NaCl)	100ml	-
20% Tween	1ml	0.02%

*Table 2.8 Composition of 1X TBS*

Reagents	Amount
Distilled H <sub>2</sub> O	900ml
10X TBS (200 mM Tris, 1.5M NaCl)	100ml

*Table 2.9 Composition of 10X TBS pH 7.6*

Reagents	Amount	Final Concentration
Distilled H <sub>2</sub> O	1000 ml	-
NaCl	88g	1.5M
Tris	24g	200 mM

*Table 2.10 Antibodies used for Western Blot Analysis*

Antibody	Raised in	Concentration used	Catalogue Number	Company
Alpha Tubulin	Mouse	1:1000	66031-1-Ig	ProteinTech
CBX2	Rabbit	1:1000	ab80044	Abcam
RBL2	Rabbit	1:1000	13610S	Cell Signalling Technology
E2F4	Rabbit	1:1000	10923-I-AP	ProteinTech
Secondary Antibody anti-mouse	Rabbit	1:1000	P0161	Dako
Secondary Antibody anti-rabbit	Goat	1:1000	P04481-2	Dako

## 2.8 Gene Expression Analysis

### 2.8.1 RNA Extraction

Cells were grown for 72 hours in a 6 well plate. After 72 hours, the media was removed from the wells. Cells were washed in 1X PBS. 350  $\mu$ l of buffer RLT from the Qiagen RNeasy Mini Kit (Qiagen, UK) was added per well. This was then transferred to DNAase/RNAase free microcentrifuge tubes. 350  $\mu$ l of 70% Ethanol was added per sample and pipetted up and down to ensure mixing. 700  $\mu$ l of the sample was transferred to RNeasy Mini spin columns in collection tubes. These were then centrifuged for 15 seconds at 8,000 x g. The spin column was removed and the liquid in the collection tube was discarded. The spin column was placed back into the collection tube and 700  $\mu$ l of buffer RW1 from the kit was added per sample. The samples were centrifuged at 8,000 x g for 15 seconds. The liquid in the collection tube was discarded. 500  $\mu$ l of buffer RPE from the kit was added per sample. The samples were centrifuged at 8,000 x g for 15 seconds. The liquid was discarded. 500  $\mu$ l of buffer RPE was added per sample. The samples were centrifuged at 8,000 x g for 2 minutes. The spin columns were transferred to new DNAase/RNAase free tubes and 30  $\mu$ l of Rnase-free water from the kit was added per column. The samples were centrifuged for 1 minute at 8,000 x g to elute the DNA. The samples were incubated at 55°C for 10 minutes. After this had been completed the concentration of RNA in ng/ $\mu$ l was calculated using a Nanodrop 2000 (Thermo Scientific, UK).

### 2.8.2 Reverse Transcription (RT)

Reverse transcription was carried out on the RNA extraction samples to create complementary DNA (cDNA). First, 1  $\mu$ g of RNA was needed, so the volume of this was calculated based on sample RNA concentration. This volume was then made up to 12.7  $\mu$ l by adding molecular grade H<sub>2</sub>O. A reverse transcription reaction mix was made containing sample plus 1 X M-MLV RT Buffer (Promega, UK), 400 $\mu$ M dNTP (Thermofisher Scientific, UK), 500 nM oligoDT (Invitrogen, UK) and 60u of M-MLV Reverse Transcriptase (Stock 200u/ $\mu$ l) (Promega, UK). Samples were then incubated at 37°C for 1 hour. After incubation, the samples were incubated at 100°C for 5 minutes to stop the reaction. The samples were pulsed down to remove any liquid from the lids of the tubes and diluted 1:10 with molecular grade H<sub>2</sub>O for use in qPCR.

### 2.8.3 Quantitative Polymerase Chain Reaction (qPCR)

For each set of primers being used in the experiment a master mix was prepared. A master mix for a single reaction contained 1X SYBR Green Mix (Sigma, UK), 1:100 final dilution of

ROX Dye (Sigma, UK), 2.1  $\mu$ l of molecular grade water, 2nM of forward primer and 2nM of reverse primer (Table 2.11). The volume of master mix prepared was adjusted to how many reactions were being carried out. 8  $\mu$ l of the master mix was pipetted into the bottom of the wells on a MicroAmp Fast Optical 96-well Reaction Plate (life technologies) and then 2  $\mu$ l of the sample was added to the side of the wells before an Optical Adhesive Coverslip (life technologies) was placed on top of the 96 well plate. The plate was then placed into a plate spinner to mix the sample and master mix together in the wells. The plate was placed into a Real-Time PCR StepOne Plus (Applied Biosystems) machine and StepOne Software was used to run the qPCR and analyse the results. For the first step of the qPCR the plate was heated at 95°C for 10 minutes. Step two occurred for 40 cycles of 95°C for 15 seconds and then 60°C for 1 minute. The final stage was 95°C for 15 seconds, 60°C for 1 minute and 95°C for 15 seconds. The data was then exported and analysed in excel. The gene expression profiling data was analysed using the delta delta CT method, this is where the cycle time (CT) mean generated from the qPCR is used to calculate relative gene expression compared to a control sample following normalisation using the expression of a chosen housekeeping gene (*RPL13A*) (Livak & Schmittgen, 2001).

Table 2.11 Primer sequences. Working concentration of primers used in qPCR was 0.05 µg/µl

Primer	Forward/Reverse	Sequence	Method	Company
RPL13A	F	CCTGGAGGAGAAGAGGAAAGAGA	Gene Expression Profiling	Sigma
RPL13A	R	TTGAGGACCTCTGTGTATTTGTCAA	Gene Expression Profiling	Sigma
CBX2	F	GCTCCAAAGCCAGACTAACA	Gene Expression Profiling	IDT
CBX2	R	CAGGGACAGACATCCTCATTTTC	Gene Expression Profiling	IDT
CCNA2	F	AGCTGCCTTTCATTTAGCACTCTAC	Gene Expression Profiling	Sigma
CCNA2	R	TTAAGACTTTCCAGGGTATATCCAGTC	Gene Expression Profiling	Sigma
PLK1	F	ATTTCCGCAATTACATGAGC	Gene Expression Profiling	Sigma
PLK1	R	TCCTGGAAGAAGTTGATCTG	Gene Expression Profiling	Sigma
AURKA	F	CCTACAAAAGAATATCACGGG	Gene Expression Profiling	Sigma
AURKA	R	CAAGTACTTCTCTGAGCATTG	Gene Expression Profiling	Sigma
CDK1	F	CCTAGCATCCCATGTCAAAAAGCTTGG	Gene Expression Profiling	Sigma
CDK1	R	TGATTCAGTGCCATTTTGCCAGA	Gene Expression Profiling	Sigma
CDK4	F	AGATTGCCCTCTCAGTGTCCTCA	Gene Expression Profiling	Sigma
CDK4	R	TGGAAGGAAGAAAAGCTGCC	Gene Expression Profiling	Sigma
RBL2	F	AGTCCAAAGCACTTAGAATC	Gene Expression Profiling	Sigma
RBL2	R	GAATCTGTTCCAGTTTCTCAC	Gene Expression Profiling	Sigma
AURKA	F	GGTGACAACAAACCCGACG	Chromatin Immunoprecipitation	IDT
AURKA	R	CCGGGTTCTTAGGGAGCAAG	Chromatin Immunoprecipitation	IDT

PLK1	F	TCAATCAGGTTTTCCCCGGC	Chromatin Immunoprecipitation	IDT
PLK1	R	TTTAAAATCCAAACCCGCCG	Chromatin Immunoprecipitation	IDT
CCNA2	F	AGTTCAAGTATCCCGCGACT	Chromatin Immunoprecipitation	IDT
CCNA2	R	GGTTTACCCTTCACTCGCCT	Chromatin Immunoprecipitation	IDT
CDK1	F	TTTCTTTCGCGCTCTAGCCA	Chromatin Immunoprecipitation	IDT
CDK1	R	CAATCGGGTAGCCCGTAGAC	Chromatin Immunoprecipitation	IDT
CDC20	F	GGTTGCGACGGTTGGATTTT	Chromatin Immunoprecipitation	IDT
CDC20	R	AGTTCCGACCGGCTTTAACA	Chromatin Immunoprecipitation	IDT
UBE2S	F	GGACCGTTTGAATGAGACGC	Chromatin Immunoprecipitation	IDT
UBE2S	R	CCCAGGAAGACCGTTAGTCG	Chromatin Immunoprecipitation	IDT
UBE2C	F	ATCCCACGTGGACGTTTTCT	Chromatin Immunoprecipitation	IDT
UBE2C	R	CGAATCCGTAGCGAATTGGTG	Chromatin Immunoprecipitation	IDT
CCNB1	F	CTGGAAACGCATTCTCTGCG	Chromatin Immunoprecipitation	IDT
CCNB1	R	GCCAGCCTAGCCTCAGATTT	Chromatin Immunoprecipitation	IDT

## 2.9 Co-Immunoprecipitation (Co-IP)

A cell suspension of 1 million cells per reaction was transferred to 15 ml falcon tubes and centrifuged for 3 minutes at 0.3 RCF. The supernatant was discarded. 500  $\mu$ l of lysis buffer (Table 2.12) was added to each pellet and pipetted up and down to ensure the pellet was re-suspended. The samples were then transferred to microcentrifuge tubes and incubated at 4°C on a rotating spinning wheel for 1 hour. After incubation, the samples were centrifuged for 3 minutes at 13.3 x g. The supernatant was transferred to new tubes and 1/10<sup>th</sup> of this supernatant was transferred to another new tube to be the input sample. The input sample was stored at -20°C. The appropriate amount of relevant antibodies for the proteins of interest were added to the samples (Table 2.13). The tubes were rotated on a spinning wheel for 2 hours at 4°C. During the incubation time, 25  $\mu$ l of Protein A Dynabeads (Invitrogen, UK) per sample were added to new microcentrifuge tubes. The beads were washed with 0.1% Triton-X 100 in 1X TBS. The tubes were then placed onto a magnetic rack to magnetise the beads and the supernatant was removed. This step was repeated two more times. A final amount of 30  $\mu$ l was added to the beads. After incubation, the beads were magnetised, and the solution was removed. The samples containing the antibodies were then added to the beads. These samples were incubated overnight on a spinning wheel at 4°C. After incubation, the samples were placed on a magnetic rack and the supernatant was transferred to a new tube and kept as the flowthrough. The beads were washed three times using the same protocol as previously. 30  $\mu$ l of SDS sample buffer was then added to the beads and 6  $\mu$ l was added to the input samples. Once the SDS buffer was added to the beads and input samples these were then used for western blot analysis (see section 2.7).

*Table 2.12 Composition of 5ml of Lysis Buffer*

Reagent	Amount	Final Concentration
Tris pH7.5 1M	250 $\mu$ l	52 mM
NaCl 4M	188 $\mu$ l	158 mM
H <sub>2</sub> O	4.315 ml	-
DTT 1M	5 $\mu$ l	1 mM
Protease Inhibitor	5 $\mu$ l	-

Table 2.13 Antibodies used for Co-IP

Antibodies	Amount added ( $\mu$ l)	Catalogue Number	Company
RBL2	4 $\mu$ l	13610S	Cell Signalling Technology
E2F4	6.6 $\mu$ l	10923-I-AP	ProteinTech
Rabbit IgG	2 $\mu$ l	C15410206	Diagenode

## 2.10 Chromatin Immunoprecipitation (ChIP)

### 2.10.1 Plating of Cells

A CBX2 knockdown was carried out on MDA-MB-231 cells. 3.5 million cells were plated into two 150 mm dishes (Sarstedt, UK), one transfected with siSCR and the other by a siRNA pool created using equal amount of siCBX2 #1/3/4. A master mix of 1000  $\mu$ l of basal media, 20  $\mu$ l of RNAiMAX and 10  $\mu$ l of siSCR (50 $\mu$ M stock) or 3.3  $\mu$ l of each siCBX2 (50 $\mu$ M stock) for the siCBX2 pool. These were incubated for 72 hours at 37°C and 5% CO<sub>2</sub>.

A CBX2 knockdown was carried out on MDA-MB-468 cells. 2.5 million cells were plated into two 100 mm dishes (Sarstedt, UK), one transfected with siSCR and the other by a siRNA pool was created using equal amount of siRNA #1/3/4. A master mix of 500  $\mu$ l of basal media, 10  $\mu$ l of RNAiMAX and 5  $\mu$ l of siSCR or 1.66  $\mu$ l of each siCBX2 for the siCBX2 pool. These were incubated for 48 hours at 37°C and 5% CO<sub>2</sub>.

### 2.10.2 Formaldehyde Fixation

After incubation, 11% Formaldehyde (Table 2.14) was added to the dishes to make a final 1% formaldehyde concentration and gently tipped to ensure mixing. The dishes were incubated at room temperature for 7 minutes. Next, 2.5M Glycine was added to the dishes to a final concentration of 125 nM to quench the formaldehyde and tipped to ensure mixing. The dishes were incubated at room temperature for 5 minutes. After incubation, the media was removed and discarded. The dishes were washed twice in cold 1X PBS. On the second wash the cells were scraped using a cell scraper and transferred to a 15 ml falcon tube. The cell suspension was then centrifuged at 2000 RCF for 4 minutes at 4°C (Hettich, Universal 32R). After the cells were spun down the supernatant was removed from the cell pellet and discarded. At this point the cell pellet could be snap frozen in liquid nitrogen and stored at -80°C or the cell lysis step could proceed immediately.

*Table 2.14 Composition of 10ml of 11% Formaldehyde solution*

Reagent	Amount	Final Concentration
HEPES-KOH 0.5M	1ml	50 mM
NaCl 4M	250 $\mu$ l	0.1 M
EDTA 0.5M	20 $\mu$ l	1 mM
EGTA 0.5M	10 $\mu$ l	500 $\mu$ M
37% Formaldehyde	3ml	11%
Molecular Grade H <sub>2</sub> O	5.27ml	-

### 2.10.3 Cell lysis and sonication

5 ml of buffer LB1 (Table 2.15) was added to the cell pellet and gently rocked on ice for 10 minutes. The cell suspension was centrifuged at 2000 RCF for 4 minutes at 4°C and the supernatant was removed. This process was repeated using buffer LB2 (Table 2.15). After the cell suspension was centrifuged and the supernatant removed, 500  $\mu$ l of buffer LB3 (Table 2.15) was added to the cell pellet and rocked on ice for 30 minutes. This was then transferred to an RNAase/DNAase free microcentrifuge tube. The cell suspension was sonicated in ice cold water (Bioruptor Sonication System UCD-200, Diagenode) for 30 minutes total in 30 seconds on and 30 seconds off intervals. After every 5 minutes of the 30-minute sonication the ice was replaced in the water bath of the sonicator to keep the samples cool. After sonication, the samples were centrifuged (Eppendorf, Centrifuge 5430 R) at 20,000 RCF at 4°C for 10 minutes and the supernatant was transferred to a new tube. The concentration of DNA in ng/ $\mu$ l was calculated using a Nanodrop 2000 so that the amount of chromatin used for each experiment could be calculated.

Table 2.15 Composition of 100ml of Lysis Buffers 1/2/3

Reagent	LB1	Final Concentration	LB2	Final Concentration	LB3	Final Concentration
HEPES-KOH 0.5M	10ml	50 mM	-	-	-	-
NaCl 4M	3.5ml	140 mM	5ml	200 mM	2.5ml	100 mM
EDTA 0.5M	200µl	1 mM	200µl	1 mM	200µl	1 mM
EGTA 0.5M	-	-	100µl	0.5 mM	100µl	0.5 mM
Molecular Grade H <sub>2</sub> O	79.05ml	-	93.7ml	-	95.6ml	-
Glycerol	10ml	10%	-	-	-	-
NP40	500µl	0.5%	-	-	-	-
Titron-X 100	250µl	0.25%	-	-	-	-
Tris HCL pH 8 1M	-	-	1ml	10 mM	1ml	10 mM
Na-deoxycholate	-	-	-	-	0.1g	0.1%
N-lauroylsarcosine	-	-	-	-	0.5g	0.5%

#### 2.10.4 Binding of antibody to magnetic beads

40 µl of Protein A DynaBeads for each CHIP reaction were added to RNAase/DNAase free microcentrifuge tubes and washed with 700 µl of 0.5% BSA in 1X PBS. 0.5% BSA in 1X PBS was passed through a sterile 0.45 µm syringe filter before use. The wash step was repeated once more by using a magnetic rack to remove the BSA from the beads in between washes. A final 700 µl of BSA was added to the beads and the appropriate amount of antibody was added to the tubes (Table 2.16). Parafilm was added to the lids of the tubes and rotated at 4°C for 6 hours. After the 6-hour bead-antibody incubation the amount of chromatin required for the experiment was calculated so that it was equal between each arm of the experiment and this sample was made up to 630 µl using LB3. 70 µl of 10% Titron-X 100 (Fisher Scientific, UK) in LB3 was added and mixed. 70 µl was then removed to be used for an input sample, this was then stored at -20°C. The BSA solution was removed from the beads using the magnetic rack and then the chromatin-LB3 suspension was added to the beads. This then was rotated overnight at 4°C.

Table 2.16 Antibodies used for CHIP

Antibody	Animal raised in	Amount ( $\mu$ l) needed for 10 $\mu$ l of chromatin	Catalogue Number	Company
Rabbit IgG	Rabbit	2 $\mu$ l	C15410206	Diagenode
RBL2	Rabbit	10 $\mu$ l	13610S	Cell Signalling Technology

#### 2.10.5 Elution and cross-link reversal

After incubation, the supernatant was removed from the beads using the magnetic rack. The beads were washed 5 times with RIPA buffer, then CHIP wash buffer (1X TBS) was added to the beads. The microcentrifuge tubes were centrifuged at 3000 RCF for 3 minutes. The wash steps were all done at 4°C. Using the magnetic rack, the CHIP wash buffer was removed from the beads and 200  $\mu$ l of elution buffer (Table 2.17) was added to the samples and the input samples. These samples were then placed on a hot block for 7 hours at 65°C to reverse crosslinks. The samples were mixed every 5 minutes for the first 15 minutes of incubation. After 7 hours the samples were pulsed down and using a magnetic rack the solution was transferred to new microcentrifuge tubes and the beads were discarded. At this point the samples could be stored at -20°C until ready for DNA purification.

Table 2.17 Composition of 50ml of Elution Buffer

Reagent	Amount	Final Concentration
Tris-HCl pH 8 1M	2.5ml	50 mM
EDTA 0.5M	1ml	10 mM
20% SDS	2.5ml	1%
H <sub>2</sub> O	44ml	-

#### 2.10.6 Protein and RNA digestion

First, 200  $\mu$ l of TE buffer (Table 2.18) was added to each sample along with RNase A (20 mg/ml) obtained from the PureLink Genomic DNA Mini Kit to a final concentration of 20  $\mu$ g/ml (Thermo Fisher Scientific, UK). These samples were then incubated at 37°C on a hot block for 30 minutes. After incubation Proteinase K was added to a final concentration of 200

µg/ml to the samples and incubated at 55°C for 1 hour. Once incubation was finished the samples were pulsed down.

*Table 2.18 Composition of 50ml of TE Buffer*

Reagent	Amount	Final Concentration
Tris-HCl 1M	500 µl	10 mM
EDTA 0.5M	100 µl	1 mM
Molecular Grade H <sub>2</sub> O	49.4ml	-

### 2.10.7 DNA Purification

DNA was purified using the PureLink Genomic DNA Mini Kit (Thermo Fisher Scientific, UK). 200 µl of Purelink Genomic Binding Buffer was added and vortexed. Next 200 µl of 100% Ethanol was added to the samples and vortexed. This solution was then transferred to spin columns in tubes. The tubes were centrifuged at 10,000 x g for 1 minute at room temperature. The columns were then transferred to new collection tubes and 500 µl of Wash Buffer 1 was added to each sample. The samples were centrifuged again at 10,000 x g for 1 minute. The columns were transferred to new collection tubes. 500 µl of Wash Buffer 2 was added to each sample and then centrifuged at 17,000 x g for 1 minute. The columns were then transferred to sterilised DNA/RNA free microcentrifuge tubes and 140 µl of molecular grade H<sub>2</sub>O was added to each sample and incubated at room temperature for 1 minute. The samples were centrifuged at 17,000 x g for 1 minute and the columns were removed from the microcentrifuge tubes, and the samples were stored at -20°C until needed qPCR analysis (section 2.8.3)

### 2.11 Cleavage Under Targets & Release Using Nuclease (CUT & RUN)

CUT & RUN is an assay that can identify areas of the genome bound by a protein of interest using a low cell number compared to ChIP. The assay works by binding cells to Concanavalin A magnetic beads and adding digitonin solution which permeabilises the cell membranes allowing the specific antibody used to enter the cells and reach the nuclei where it can bind to the protein of interest. pAG-MNase is added which binds to the antibody via the pAG part of the enzyme and the MNase is activated by the calcium ions from calcium chloride to digest the DNA either side of where the antibody is bound to its target on the chromatin. The chromatin can then be purified using spin columns and analysed via qPCR or sent for next generation sequencing (Cell Signaling Technology, 2022).

### 2.11.1 Cell Preparation and Binding of Primary Antibody

CUT & RUN was performed using a CUT & RUN assay kit (Cell Signalling Technologies). 200X Protease Inhibitor Cocktail (PIC) and 100X Spermidine were warmed and thawed before use. Digitonin Solution was warmed at 90°C for 5 minutes until fully thawed and then put onto ice. The Concanavalin A Bead Activation Buffer was also put onto ice. 2 ml of 1X Wash Buffer was made up per sample plus an additional 100 µl for each reaction or input sample. An excess of half a reaction was added to the mix. For example, for 2.5 ml of 1X Wash Buffer, 250 µl of 10X Wash Buffer, 25 µl of 100X Spermidine, 12.5 µl of 200X PIC and 2212.5 µl of water were added and then equilibrated to room temperature. To make the Antibody Binding Buffer mix, 1 µl of 100X Spermidine, 0.5 µl of 200X PIC, 2.5 µl of Digitonin Solution and 96 µl of Antibody Binding Buffer was prepared for each reaction and then placed on ice. The Concanavalin A Magnetic Beads were resuspended by pipetting up and down. 10 µl of beads per sample were transferred to a new tube. 100 µl of Concanavalin A Bead Activation Buffer was added per 10 µl of beads and pipetted up and down to mix. The tube was then placed on a magnetic rack and the solution was removed once it turned clear. This wash step was repeated a second time and a final volume of Concanavalin A Bead Activation Buffer equal to the initial volume of bead suspension was added to the beads and placed on ice.

Cells were then trypsinised and counted. 100,000 cells were collected for each reaction including an extra 100,000 cells for the input sample. The cell suspension was then centrifuged for 3 minutes at 600 x g at room temperature and the liquid was discarded. The cell pellet was resuspended in 1 ml of 1X Wash Buffer at room temperature and mixed by pipetting up and down. This was then centrifuged at 600 x g for 3 minutes and the liquid was removed, and this wash step was repeated one more time. A final 100 µl of 1X Wash Buffer was added per 100,000 cells and the cell pellet was resuspended by pipetting up and down. 100 µl of the cells were transferred to a new tube for the input sample and stored at -20°C. The Concanavalin A beads were resuspended and 10 µl of beads were added per 100,000 cells to the washed cell suspension. The cell:bead suspension was then rotated on a spinning wheel at room temperature for 5 minutes. After this the samples were centrifuged at 100 x g to remove any cell:bead suspension from the lid of the tube. The tubes were then placed on a magnetic rack and once the beads were magnetised the liquid was removed. 100 µl of Antibody Binding Buffer mix was added per 100,000 cells and the tube was placed on ice. 100 µl of the cell:bead suspension was aliquoted into separate 1.5 ml tubes for each reaction

and placed back on ice. Relevant antibodies (Table 2.19) for the proteins or histone marks to be analysed were added and mixed by pipetting up and down. The tubes were then rotated on a spinning wheel at 4°C for 2 hours.

*Table 2.19 Antibodies used for CUT & RUN*

Antibody	Amount used	Catalogue Number	Company
CBX2	2 µl	ab80044	Abcam
CBX2	2 µl	C15410339	Diagenode
Tri-Methyl-Histone H3 (Lys4)	2 µl	9751T	Cell Signaling Technology
Rabbit (DA1E) mAb IgG XP Isotype Control	5 µl	66362S	Cell Signaling Technology

### 2.11.2 Binding of pAG-MNase Enzyme

1.05 ml of Digitonin Buffer was prepared per reaction by adding 105 µl of 10X Wash Buffer, 10.5 µl of 100X Spermidine, 5.25 µl of 200X PIC, 26.25 µl of Digitonin Solution and 903 µl of water. As well as this, a pAG-MNase pre-mix was made by adding 50 µl of Digitonin Buffer and 1.5 µl of pAG-MNase Enzyme per reaction. This pre-mix was then placed on ice. After the 2 hour incubation the tubes were centrifuged at 100 x g to remove any cell:bead suspension from the lids of the tubes. The tubes were placed on a magnetic rack and the solution was removed. 1 ml of Digitonin Buffer was added to each tube and mixed by pipetting up and down. The tubes were placed back on the magnetic rack and the once the beads were magnetised the buffer was removed. 50 µl of pAG-MNase pre-mix was added to each tube and mixed. The tubes were then rotated on a spinning wheel at 4°C for 1 hour.

### 2.11.3 DNA Digestion and Diffusion

2.15 ml of Digitonin Buffer was prepared for each reaction by adding 215 µl of 10X Wash Buffer, 21.5 µl of 100X Spermidine, 10.75 µl of 200X PIC, 53.75 µl of Digitonin Solution and 1.849 ml of water. In addition to this, 150 µl of 1X Stop Buffer was prepared for each reaction by adding 37.5 µl of 4X Stop Buffer, 3.75 µl of Digitonin Solution, 0.75 µl of RNase A, 5 µl of Spike-In DNA (diluted 500-fold by adding 1 µl of Spike-In DNA to 199 µl of molecular grade H<sub>2</sub>O) and 108 µl of molecular grade H<sub>2</sub>O. The Calcium Chloride was

placed on ice. The samples were centrifuged at 100 x g to remove any cell:bead suspension from the lids. The tubes were placed on the magnetic rack and the solution was removed once the beads had magnetised. 1 ml of Digitonin Buffer was added to the tubes. The beads were re-magnetised on the rack so the buffer could be removed, and the beads were washed again in 1 ml of Digitonin Buffer. The tubes were placed back on the rack and after the beads were magnetised a final volume of 150 µl of Digitonin Buffer was added to the tubes. The tubes were then incubated at 4°C for 5 minutes to allow cooling before digestion. After the incubation 3 µl of cold Calcium Chloride was added to each tube and mixed by pipetting up and down. The samples were incubated at 4°C for 30 minutes. After incubation 150 µl of 1X Stop Buffer was added to each tube and mixed by pipetting up and down. The samples were then incubated at 37°C for 10 minutes. Once the incubation was finished the samples were centrifuged at 4°C for 2 minutes at 16,000 x g and then the beads were magnetised on a magnetic rack. The supernatant was transferred to a new 1.5 ml tube and placed on ice, or this can be a safe stop where the samples can be stored at -20°C.

#### 2.11.4 Preparation of the Input Sample

DNA Extraction Buffer was warmed before use. 2 µl of Proteinase K, 0.5 µl of RNase A and 197.5 µl of DNA Extraction Buffer was prepared per input sample. 200 µl of this mix was then added to the input sample and mixed by pipetting up and down. The sample was incubated at 55°C for 1 hour with shaking. After incubation, the sample was placed on ice to cool down. The sample was then sonicated (Bioruptor Sonication System UCD-200, Diagenode) in ice cold water for 30 minutes in 5-minute intervals with 30 seconds on and 30 seconds off. After sonication, the sample was centrifuged at 17,000 x g for 10 minutes at 4°C and then the supernatant was transferred to a new 1.5 ml tube.

#### 2.11.5 DNA Purification

DNA was purified using the DNA Purification Buffers and Spin Columns kit (Cell Signalling Technologies, UK). 1.5 ml of DNA Binding Buffer was added to each input and enriched chromatin sample and vortexed briefly. 600 µl of each sample was transferred to a new DNA spin column in a collection tube. The samples were then centrifuged at 17,000 x g for 30 seconds. The spin column was removed from the collection tube and the liquid was discarded. The column was put back into the collection tube. This step was repeated until the entire sample had been spun through the spin column. 750 µl of DNA Wash Buffer was then added to each spin column and centrifuged at 17,000 x g for 30 seconds. The spin column was removed, and the liquid was discarded from the collection tube. The spin column was

placed back in the collection tube. The samples were centrifuged again at 17,000 x g for 30 seconds to remove any residual Wash Buffer. The collection tube was then discarded with the liquid. 50 µl of Elution Buffer was added to each spin column and then placed into a new DNAase/RNAase free 1.5 ml tube. The samples were centrifuged at 17,000 x g for 30 seconds. The spin column was discarded and the new tubes containing the samples were stored at -20°C until used for qPCR and sequencing.

#### 2.11.6 Qubit DNA quantification

Before CUT & RUN samples were sent for sequencing, they were quantified using a Qubit 1X dsDNA HS Assay Kit (Invitrogen, UK). This was done to provide an accurate detection of the DNA concentration (ng/µl) in the samples. First, each standard was diluted 1:20 with the working solution from the kit. These were then mixed. Samples were diluted 1:200 with working solution and mixed. The samples and standards were then incubated at room temperature for 2 minutes. The Qubit was calibrated with standard 1 and then standard 2. After calibration, the samples were then analysed using the Qubit. If the concentration of the sample is too low the volumes of sample and working solution can be adjusted. 1-20 µl of sample can be added to a new tube and then made up to 200 µl with working solution and then analysed again.

#### 2.12 Statistical Analysis

A student's T test was used for the analysis of cell count data, SRB assay data, gene expression profiling data and RBL2 enrichment data.

## Chapter 3 Results

### 3.1 Knockdown of CBX2 reduces cell growth in the MDA-MB-468 cell line

Previous data has shown that after knockdown of CBX2 there was reduced cell growth in the TNBC cell line MDA-MB-231. To see if this effect would be repeated in another TNBC cell line a cell growth assay was done using MDA-MB-468 cells. The MDA-MB-468 cell line was transfected with siSCR or siCBX2 #1/3/4. The cells were grown for 96 hours before the cells were trypsinised and counted (Figure 3.1). Figure 3.1 shows the mean cell number relative to cell numbers in siSCR transfected cells for each transfection (n=4). A student's T test was carried out to compare cell numbers after CBX2 knockdown. siCBX2 #1 showed a 32.9% reduction in cell number with a p value of 0.0463. siCBX2 #3 showed a 35.4% reduction with a p value of 0.0007 and siCBX2 #4 showed a 58.1% reduction with a p value of 0.0001. The cell counts for all 3 siRNAs were lower than the siSCR and were statistically significant thus showing decreased cell number in MDA-MB-468 cells following CBX2 knockdown.

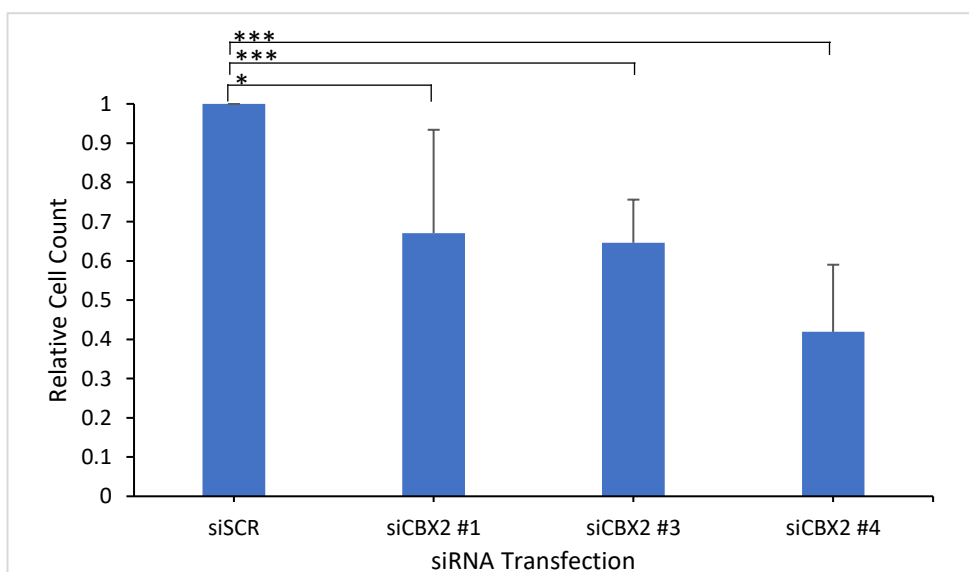


*Figure 3.1 Relative cell counts in MDA-MB-468 cells following CBX2 knockdown*

MDA-MB-468 cells were transfected with a non-silencing control (siSCR) or one of 3 CBX2 targeting siRNAs (#1/3/4) and grown for 96 hours. After 96 hours the cells were trypsinised and counted. Error bars show standard deviation (n=4). siCBX2 #1/3/4 cell numbers are relative to siSCR cell numbers. A student's T test was used to compare numbers in siCBX2 transfected cells with siSCR transfected cells. \* =  $p < 0.05$ , \*\*\* =  $p < 0.001$ .

Another cell growth assay was used to further validate the effect on cell growth after the knockdown of CBX2 in the MDA-MB-468 cell line. The MDA-MB-468 cell line was transfected with siSCR or siCBX2 #1/3/4. The cells were grown for 96 hours. An SRB assay was carried out on the cells which works by SRB binding to the proteins in cultured cells, which is solubilised, and the absorbance of the SRB measured. The absorbance of the SRB is representative of the number of cells present in the sample (Abcam, 2022). The samples were analysed with a plate reader (Figure 3.2). A student's T test was carried out to compare the absorbance after CBX2 knockdown. Figure 3.2 shows the mean results for each CBX2 targeting siRNA relative to the absorbance reading for siSCR transfected cells (n=3). siCBX2 #1 showed a 12.7% reduction in absorbance. siCBX2 #3 showed a 18.8% reduction and siCBX2 #4 showed a 35.1% reduction in absorbance. The results show that in the siCBX2 conditions there was a decrease in cell growth which mirrors the trend seen by the cell count assay, however, this decrease was not statistically significant.

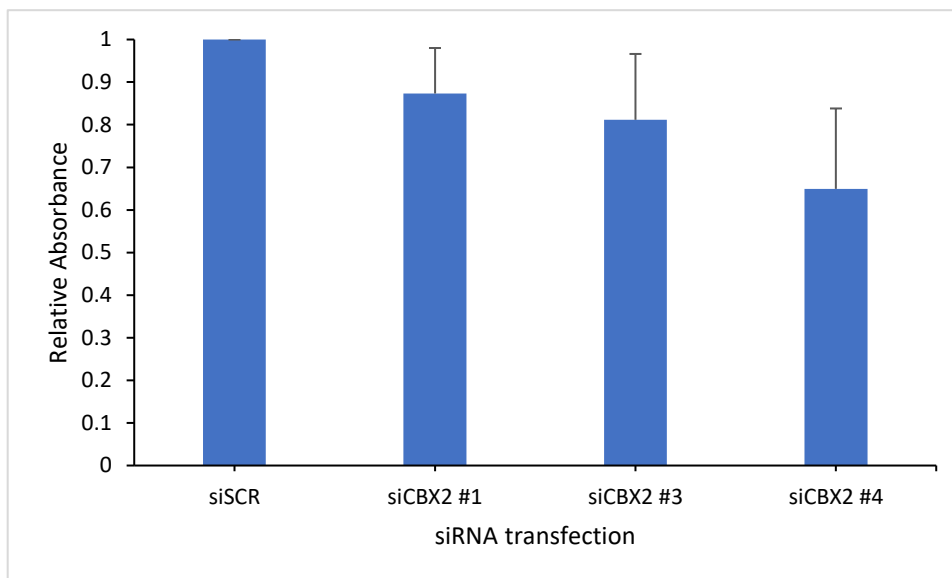


*Figure 3.2 SRB assay following the knockdown of CBX2 in MDA-MB-468 cells*

MDA-MB-468 cells were transfected with siSCR or siCBX2 #1/3/4 and grown for 96 hours. After 96 hours an SRB assay was carried out. Error bars show standard deviation (n=3). Absorbance of SRB in siCBX2 #1/3/4 transfected cells is relative to absorbance in siSCR transfected cells. A student's T test was used to compare absorbances in siCBX2 transfected cells with siSCR transfected cells

### 3.2 Gene expression profiling after CBX2 knockdown in MDA-MB-468 cells

RNA-sequencing analysis has shown that *RBL2* gene expression increased in the TNBC cell line MDA-MB-231 following the knockdown of *CBX2*. To see whether this affect was seen in another TNBC cell line, gene expression profiling was carried out on MDA-MB-468 cells to see if *RBL2* expression was affected after *CBX2* knockdown. MDA-MB-468 cells were transfected with one of 3 *CBX2* targeting siRNAs (siCBX2 #1/3/4) or a non-silencing control siRNA (siSCR). The cells were grown for 72 hours. After 72 hours an RNA extraction was carried out on the cells. After this a Reverse Transcription of 1ug of RNA was carried out and then the samples were analysed by qPCR. Primers specific for the following genes were analysed: *CBX2*, *RBL2* and *RPL13A*. *RPL13A* was used as a housekeeping control gene in order to normalise the expression of the other genes across each sample. The combined results of 4 independent experiments are shown in Figure 3.3. Results are mean expression relative to siSCR transfected cells and a student's T test was carried out to test the effect of *CBX2* knockdown compared with siSCR transfected cells. Figure 3.3A shows that for all three *CBX2* targeting siRNAs the mRNA expression of *CBX2* decreased. siCBX2 #1 decreased by 1.44 fold, siCBX2 #3 decreased by 2.82 fold and siCBX2 #4 decreased by 6.48 fold. siCBX2 #1/3/4 were significantly reduced ( $p < 0.05$ ), showing that *CBX2* was successfully knocked down in all conditions. Figure 3.3B shows that after knockdown of *CBX2* by siCBX2 #1, *RBL2* was upregulated by 3.51 fold and for siCBX2 #3 *RBL2* was upregulated by 2.05 fold. However, siCBX2 #4 showed an unexpected 2.33 fold decrease in *RBL2* expression. All siCBX2 showed statistical significance. siCBX2 #1 had a p value of 0.0138, siCBX2 #3 had a p value of 0.0172 and siCBX2 #4 had a p value of 0.0371.

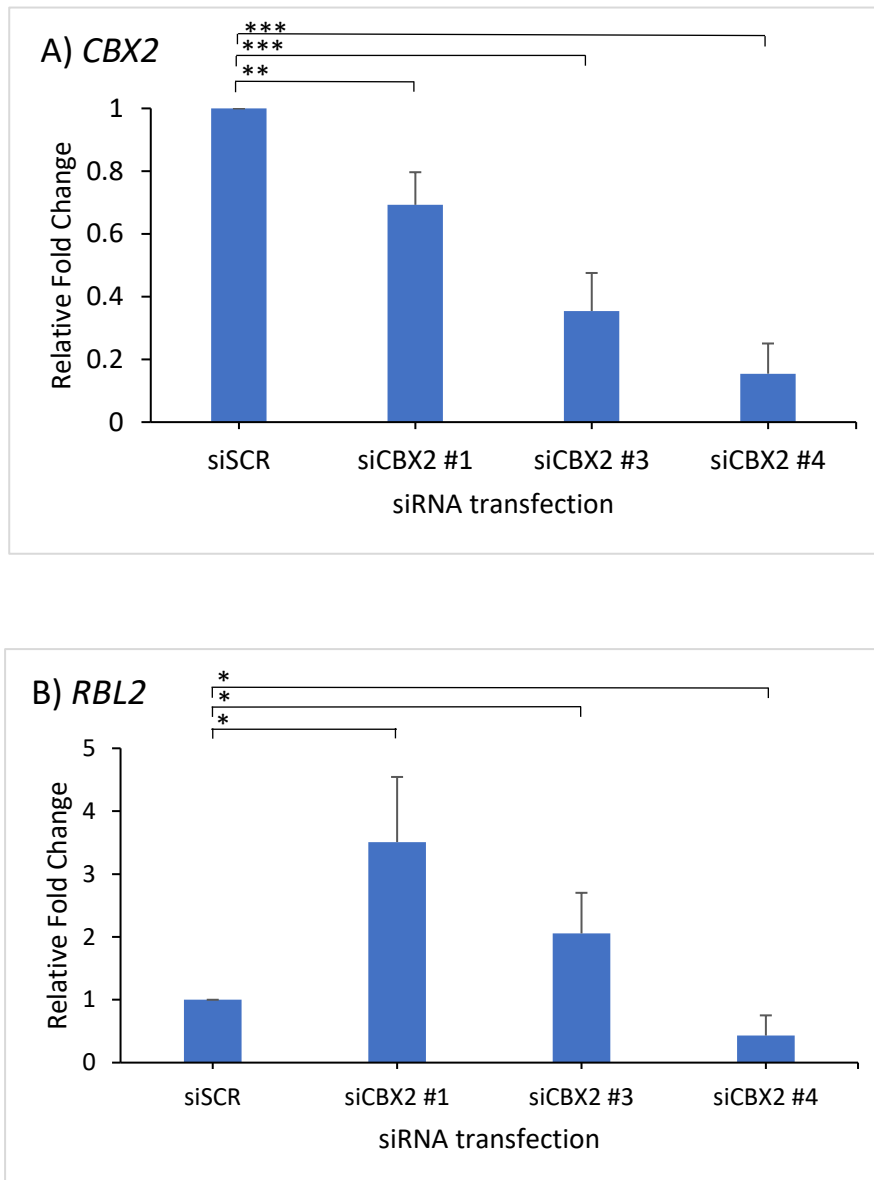


*Figure 3.3 Gene expression profiling after CBX2 knockdown in MDA-MB-468 cells*

MDA-MB-468 cells were transfected with a non-silencing control (siSCR) or one of three CBX2 targeting siRNAs (#1/3/4) and grown for 72 hours. After 72 hours an RNA extraction was carried out on the cells and then a Reverse Transcription was carried out. The samples were then used for qPCR with primers specific for *CBX2*, *RBL2* and *RPL13A*. *RPL13A* was analysed as a housekeeping gene to normalise expression across the different samples. The siSCR control data was made relative to 1 and the relative fold change of each siCBX2 was calculated against siSCR. Error bars are for Standard Deviation (n=3). A student's T test was used to compare expression with siSCR transfected cells. \* = p<0.05, \*\* = p<0.01, \*\*\* = p<0.001.

### 3.3 RBL2 and E2F4 protein expression after CBX2 knockdown in MDA-MB-231 and MDA-MB-468 cells

The previous gene expression profiling in MDA-MB-468 cells showed an increase in *RBL2* expression after CBX2 knockdown with siCBX2 #1 and siCBX2 #3. However, there was an unexpected decrease in *RBL2* expression after CBX2 knockdown using siCBX2 #4. To confirm whether this would be seen at the protein level a western blot analysis was carried out. The MDA-MB-231 and MDA-MB-468 cell line was transfected with one of 3 CBX2 targeting siRNAs (siCBX2 #1/3/4) or a non-silencing control (siSCR). The cells were grown for 72 hours before the protein was harvested and the expression of  $\alpha$ -tubulin, CBX2, RBL2 and E2F4 was assessed by western blot (Figure 3.4 and Figure 3.5). E2F4 was analysed as it is another component of the DREAM complex which RBL2 interacts with to repress E2F-target gene expression. The presence of the CBX2 band in the siSCR transfected and the absence of the CBX2 band in the siCBX2 transfected cells shows the successful knockdown of CBX2 (Figure 3.4 and Figure 3.5). RBL2 protein expression was also elevated in the siCBX2 transfected cells compared to the siSCR transfected cells indicated by a more intense protein band. This indicates that the knockdown of CBX2 increases RBL2 expression. Figure 3.4 and Figure 3.5 shows that the knockdown of CBX2 had no discernible effect on E2F4 expression. However, in Figure 3.4 the presence of E2F4 in the siCBX2 #1 band looks less compared to the other transfected conditions. This was repeated and no change was seen for the siCBX2 #1 transfected cells.  $\alpha$ -tubulin was used as a loading control to observe that the loading of the protein lysates was relatively equal across the samples.

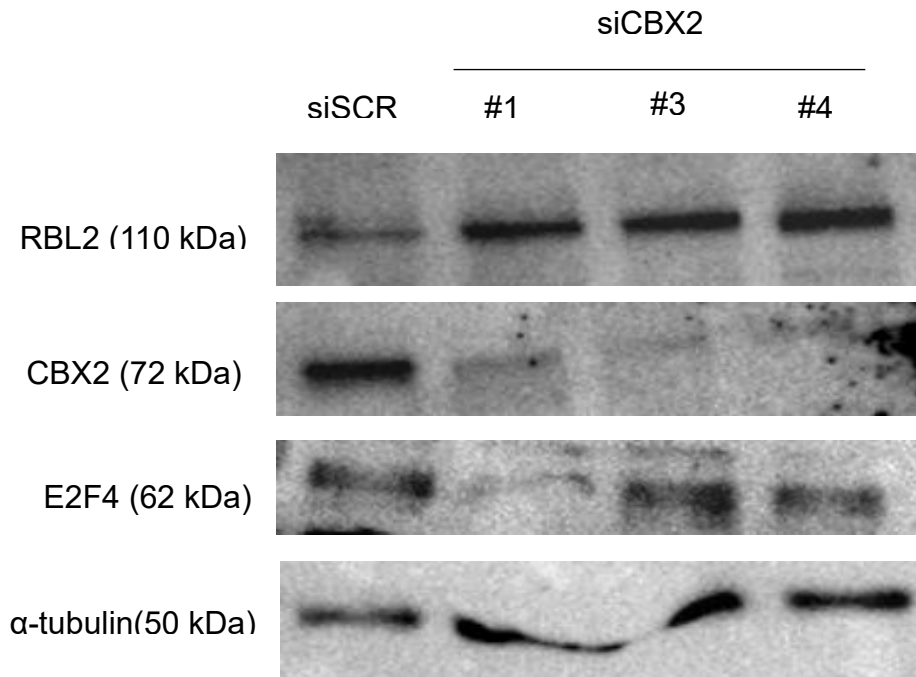


*Figure 3.4 Knockdown of CBX2 causes upregulation of RBL2 and has no effect on E2F4 expression in MDA-MB-231 cells*

MDA-MB-231 cells were transfected with a non-silencing control (siSCR) or one of 3 *CBX2* targeting siRNAs (#1/3/4) and grown for 72 hours. After 72 hours the cells were harvested in RIPA buffer and protein quantified by BCA assay. Equal amounts of protein lysate were then probed for  $\alpha$ -tubulin, *CBX2*, *RBL2* and *E2F4*. The molecular weights for each protein are included on the left of the appropriate western blot image. Which lysate is from which transfection condition is shown above the appropriate lanes. The figure is a representative image from n=4 experiments.

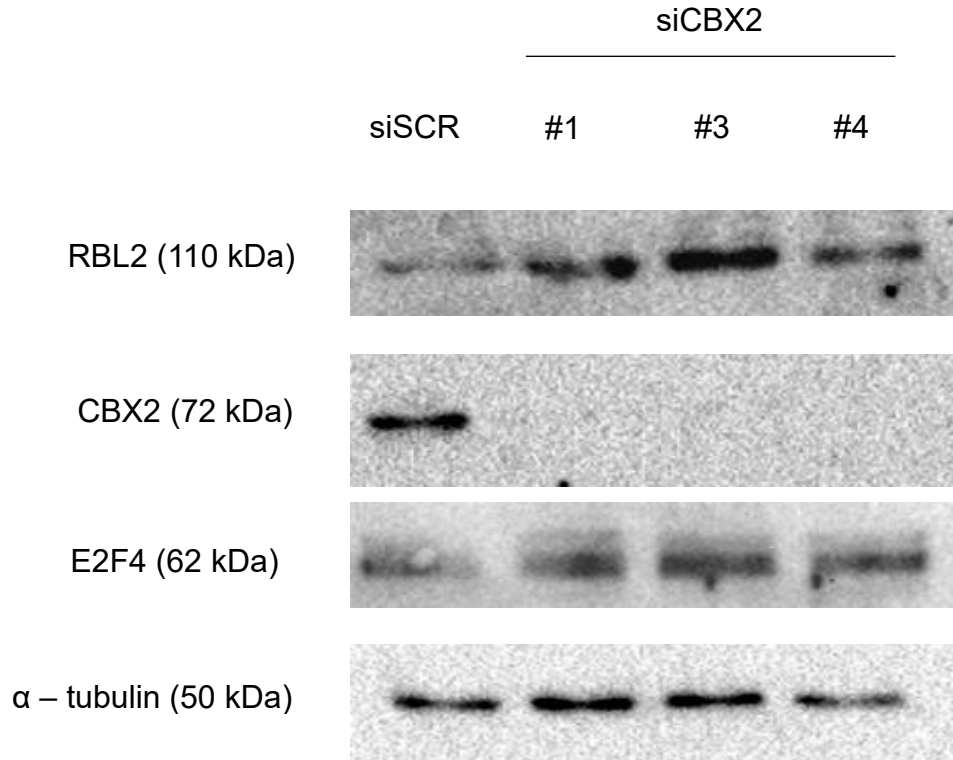


*Figure 3.5 Knockdown of CBX2 causes upregulation of RBL2 and has no effect on E2F4 expression in MDA-MB-468 cells*

MDA-MB-468 cells were transfected with siSCR or siCBX2 #1/3/4 and grown for 72 hours. After 72 hours the cells were harvested in RIPA buffer and protein quantified by BCA assay. Equal amounts of protein lysate were then probed for  $\alpha$ -tubulin, CBX2, RBL2 and E2F4. The molecular weights for each protein are included on the left of the appropriate western blot image. Which lysate is from which transfection condition is shown above the appropriate lanes. The figure is representative image of n=3 experiments.

### 3.4 Gene expression profiling shows that knockdown of CBX2 affects RBL2 target genes in MDA-MB-468 cells

After knockdown of CBX2, western blot analysis showed that RBL2 protein expression was increased in TNBC cell lines. Gene expression profiling was carried out to see if this effect affected RBL2 target genes. MDA-MB-468 cells were transfected with one of two CBX2 targeting siRNAs (siCBX2 #3/4) or a non-silencing control siRNA (siSCR). It was decided to not use siCBX2 #1 due to limited resources and it was not as effective at knocking down CBX2 as siCBX2 #3 and siCBX2 #4. The cells were grown for 72 hours followed by an RNA extraction. After this a Reverse Transcription of 1ug of RNA was carried out and then the samples were analysed through qPCR. Primers specific for the following genes were analysed: *PLK1*, *AURKA*, *CCNA2*, *CDK1* and *RPL13A*. *RPL13A* was used as a housekeeping control gene in order to normalise the expression of the other genes across each sample. The combined results of 4 independent experiments are shown in Figure 3.6. Results are mean expression relative to siSCR transfected cells and a student's T test was carried out to test the effect of CBX2 knockdown compared to siCBX2 transfected cells. *PLK1* (Figure 3.6A) and *AURKA* (Figure 3.6B) are both RBL2 target genes and are repressed by RBL2-associated DREAM-complex. For *PLK1*, knockdown by siCBX2 #3 decreased expression by 2.85 fold and knockdown by siCBX2 #4 decreased expression by 5.77 fold. For *AURKA* knockdown by siCBX2 #3 decreased expression by 1.68 fold and knockdown by siCBX2 #4 decreased expression by 2.58 fold. Both siCBX2 conditions for both genes showed no statistical significance. *CCNA2* and *CDK1* are genes that play a role in the cell cycle and are also targets of the RBL2-associated DREAM complex. It has previously been seen that after CBX2 knockdown in MDA-MB-231 cells these genes are downregulated. Figure 3.6C shows that knockdown by siCBX2 #3 decreased *CCNA2* expression by 1.64 fold with a p value of 0.0022 and knockdown by siCBX2 #4 decreased expression 1.73 fold with a p value of 0.0037. Both siCBX2 conditions were very statistically significant thus *CCNA2* has been downregulated following CBX2 knockdown. On the other hand, for *CDK1* (Figure 3.6D) expression did not change after CBX2 knockdown.

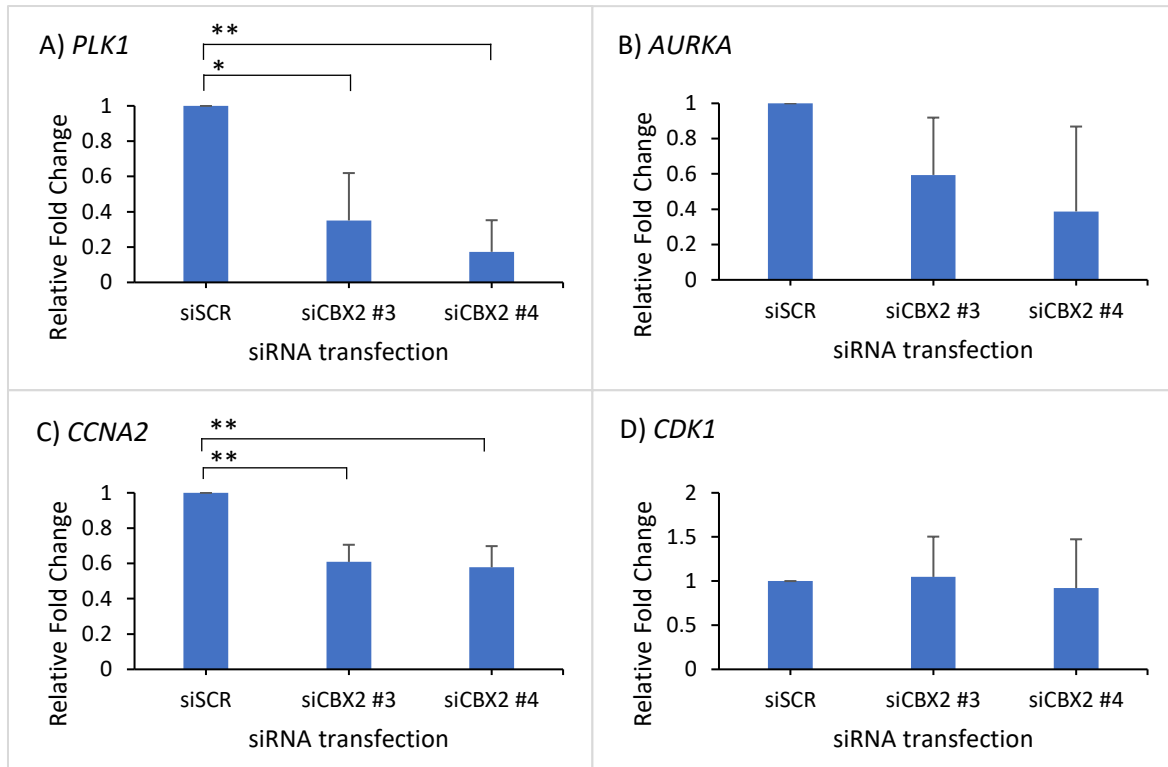


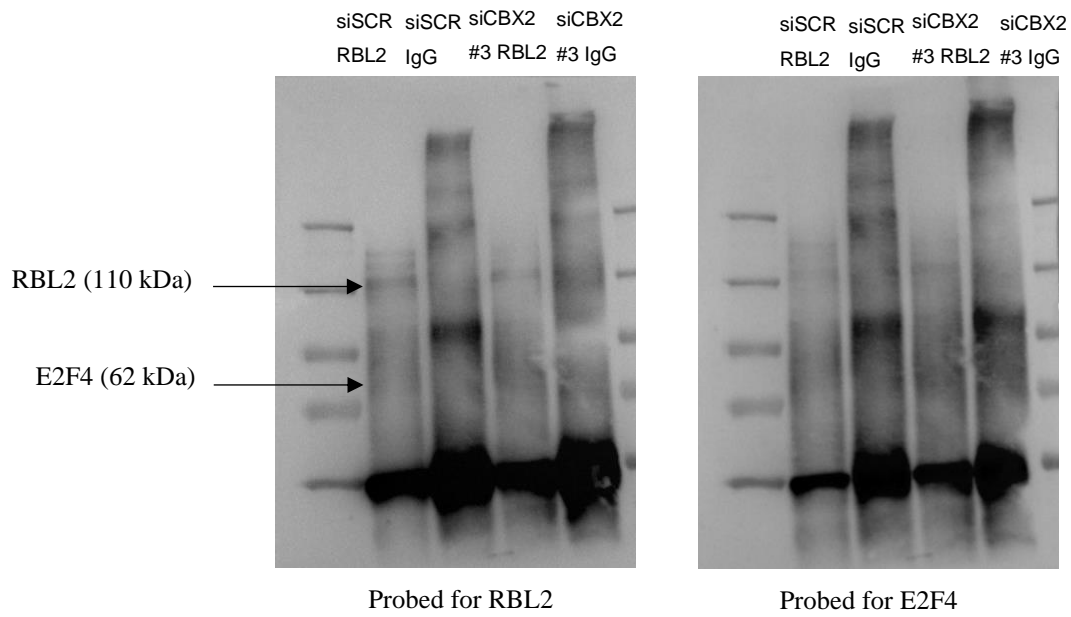
*Figure 3.6 Gene expression profiling after CBX2 knockdown affects RBL2 target genes in MDA-MB-468 cells*

MDA-MB-468 cells were transfected with a non-silencing control (siSCR) or one of two CBX2 targeting siRNAs (#3/4) and grown for 72 hours. After 72 hours an RNA extraction was carried out on the cells and then a Reverse Transcription was carried out. The final samples were then used for qPCR with primers specific for *PLK1*, *AURKA*, *CCNA2*, *CDK1* and *RPL13A*. *RPL13A* was analysed as a housekeeping gene to normalise expression across the different samples. The siSCR control data was made relative to 1 and the relative fold change of each siCBX2 was calculated against siSCR. Error bars are for Standard Deviation (n=3). A student's T test was used to compare expression with siSCR transfected cells. \* =  $p < 0.05$ , \*\* =  $p < 0.01$ , \*\*\* =  $p < 0.001$ .

### 3.5 RBL2 and E2F4 co-immunoprecipitation following CBX2 knockdown on MDA-MB-468 cells

Previous western blots and gene expression data showed an increase in RBL2 expression after knockdown of CBX2 and decrease in expression of a sub-set of RBL2 target genes. However, western blot analysis showed that E2F4 expression remained the same after knockdown of CBX2. Co-IP assays were carried out to see if the increase in RBL2 expression caused by the knockdown of CBX2 would increase RBL2 and E2F4 binding, which would indicate an increase in the formation of the DREAM complex. The MDA-MB-468 cell line was transfected with siCBX2 #3 or non-silencing control siRNA (siSCR). After incubation, the cells were harvested, and two different co-IPs were carried out. An RBL2 IP using an anti-RBL2 antibody and an IgG control antibody as well as an E2F4 IP using an anti-E2F4 antibody and an IgG control antibody. After the IP a western blot analysis was carried out. Figure 3.7A showing the RBL2 IP followed by RBL2 immunoblot shows the presence of the RBL2 band in both siSCR transfected cells and siCBX2 #3 transfected cells. No band was present in the IP using the IgG control antibody. However, no band was detected for E2F4 following immunoblot with an E2F4 antibody. For the E2F4 IP (Figure 3.7B) an RBL2 band was present in the siSCR transfected cells, and a potentially more intense band was present in the siCBX2 #3 transfected cells, when probed for RBL2. There was however no band present for E2F4 in both the siSCR transfected cells and the siCBX2 #3 transfected cells when probed for E2F4. The E2F4 IP result may therefore suggest that interaction between E2F4 and RBL2 was elevated, due to the increase in intensity of the RBL2 band, however we could not confirm whether the E2F4 IP had been successful as we were never able to detect E2F4 protein following the IP.

A)



B)

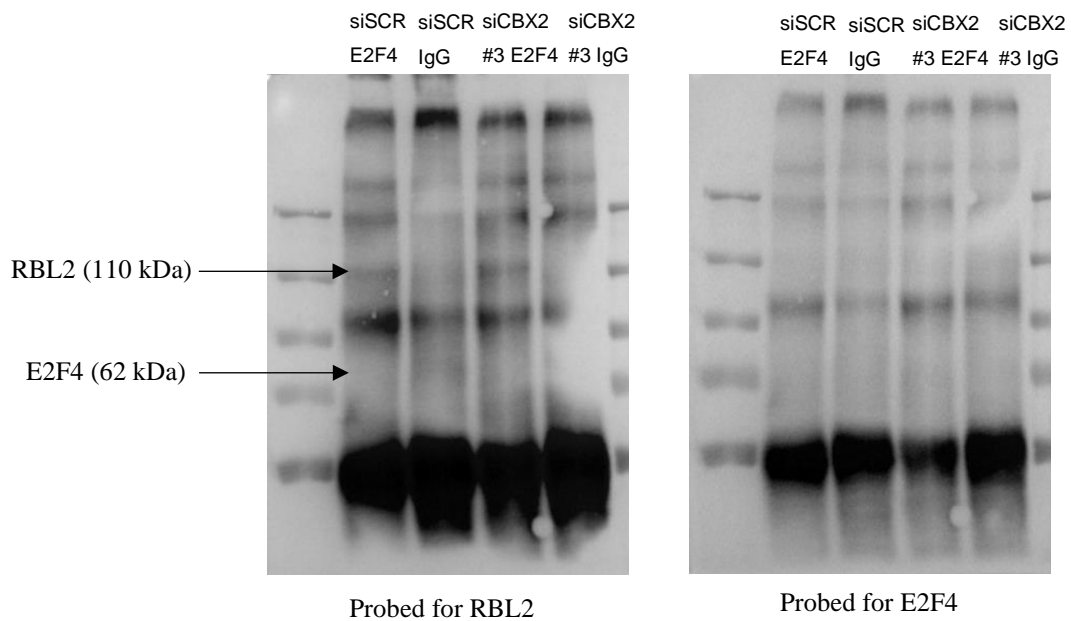


*Figure 3.7 RBL2 and E2F4 IP on MDA-MB-468 cells after knockdown of CBX2*

MDA-MB-468 cells were transfected with a non-silencing control (siSCR) or siCBX2 targeting siRNA #3 and 1 million cells were grown for 72 hours in a large dish. After incubation the cells were harvested for an RBL2 IP (A) and an E2F4 IP (B). After IP, a western blot analysis was carried out. The samples were probed for RBL2 and E2F4. The molecular weights for each protein are included on the left of the appropriate western blot image. Which lysate is from which transfection condition is shown above the appropriate lanes. RBL2 n = 3 and E2F4 n = 6.

### 3.6 Enrichment of *RBL2* at *RBL2* target gene promoters following knockdown of *CBX2* in MDA-MB-231 cells

Previous results showed that knockdown of *CBX2* increased *RBL2* protein expression and reduced the expression of *RBL2*-associated DREAM complex target genes. To see if upregulation of *RBL2* had a direct effect on target gene expression, the enrichment of *RBL2* at *RBL2* target gene promoters was assessed by ChIP. MDA-MB-231 cells were transfected with either an siRNA pool of si*CBX2* #1/3/4 or siSCR and grown for 48 hours. After incubation a ChIP was carried out using an anti-*RBL2* antibody and *RBL2* enrichment was compared between siSCR and si*CBX2* transfected cells. qPCR analysis was used to analyse the enrichment of *RBL2* at promoter sites of the following *RBL2* target genes *AURKA*, *PLK1*, *CCNA2*, *CDK1*, *CDC20*, *UBE2S*, *CCNB1*, *UBE2C*. A student's T test was used to determine if changes in enrichment were significant following *CBX2* knockdown. *RBL2* enrichment at the *CCNA2* promoter site was increased by 1.87-fold with a p value of 0.0201 (Figure 3.8A) and at the *CDC20* promoter site it was decreased by 2.28-fold with a p value of 0.0481 (Figure 3.8B). Both were statistically significant. Figure 3.8C shows that *RBL2* enrichment was increased at the *CCNB1* promoter site by 2.91-fold. Figures 3.8D and 3.8E show an increase at the *AURKA* promoter site by 4.35-fold and at the *PLK1* promoter site by 3.59-fold. Figures 3.8F, 3.8G and 3.8H for *CDK1*, *UBE2S* and *UBE2C* showed no change in *RBL2* enrichment at these sites.

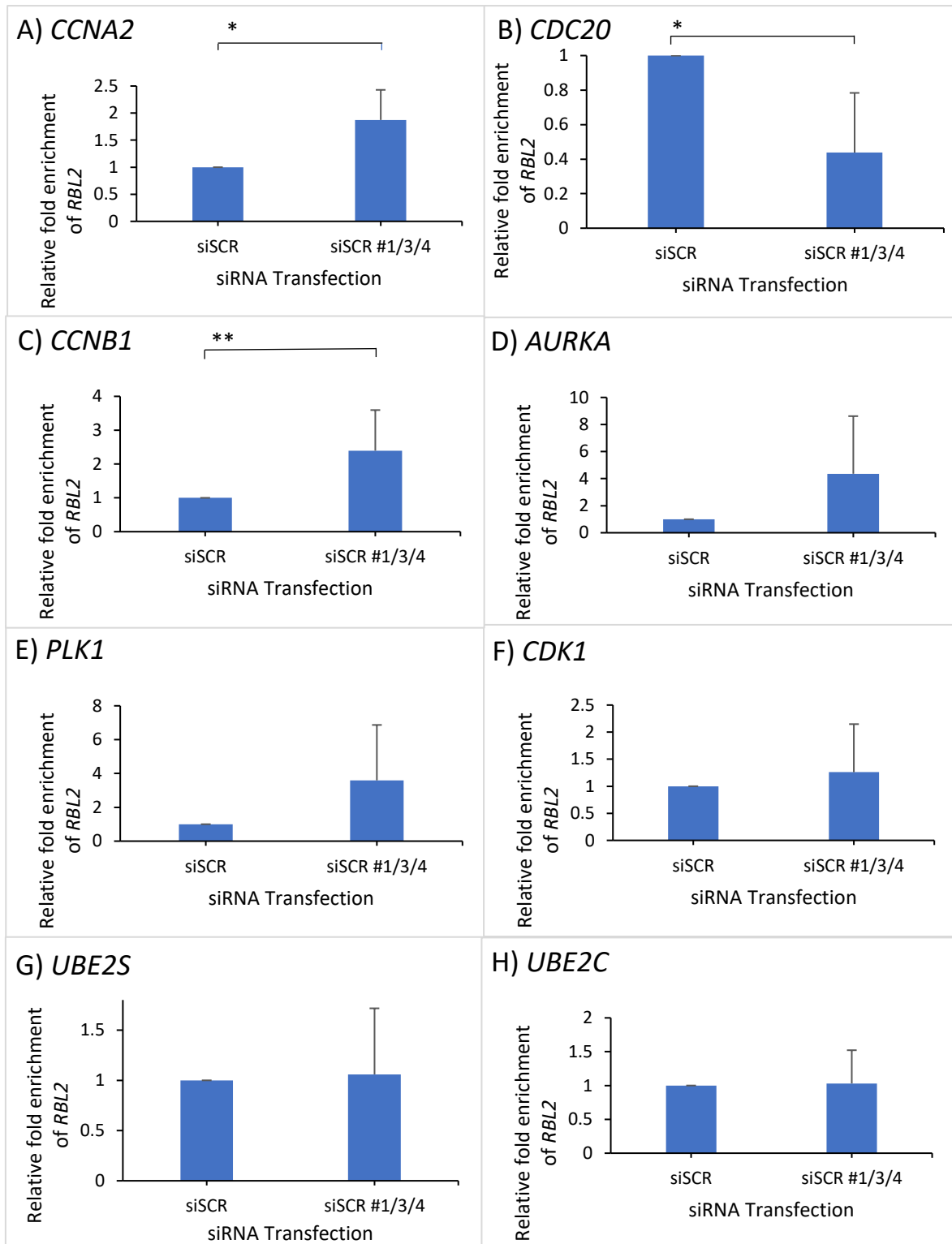


Figure 3.8 Relative fold enrichment of RBL2 at RBL2 promoter sites in MDA-MB-231 cells

MDA-MB-231 cells were transfected with either an siRNA pool of siCBX2 #1/3/4 or one a non-silencing control siRNA (siSCR). 3.5 million cells were plated onto a large dish and the cells were grown for 48 hours. After incubation a ChIP was carried out using an anti-RBL2 antibody. Enrichment was calculated as percentage input following CBX2 knockdown and was made relative to percentage input in siSCR transfected cells. Error bars represent standard deviation. A Student's T test was carried out. *AURKA*, *PLK1*, *CDC20*, *UBE2S*, *CCNB1* n=3. *CCNA2*, *CDK1*, *UBE2C* n=4.

### 3.7 Enrichment of *RBL2* at *RBL2* target gene promoters following the knockdown of *CBX2* in MDA-MB-468 cells

To assess the effect in a different TNBC cell line MDA-MB-468 cells were transfected with either an siRNA pool of siCBX2 #1/3/4 or siSCR and grown for 72 hours. After incubation, a ChIP was carried out using an anti-*RBL2* antibody and *RBL2* enrichment was compared between siSCR and siCBX2 pool transfected cells. qPCR analysis was used to analyse the enrichment of *RBL2* at the sites of the following *RBL2* target genes *AURKA*, *PLK1*, *CCNA2*, *CDK1*, *CCNB1*, *UBE2C*. A student's T test was used to determine if changes in enrichment were significant following *CBX2* knockdown. All *RBL2* target genes showed increased *RBL2* enrichment at the promoter sites following *CBX2* knockdown (Figure 3.9). *RBL2* enrichment at the *CCNA2* promoter site was increased by 1.52-fold with a p value of 0.0263 (Figure 3.9A) and at the *UBE2C* promoter site it was increased by 1.31-fold with a p value of 0.0314 (Figure 3.9B). Figure 3.9C showed that *RBL2* enrichment was increased at the *AURKA* promoter site increased by 1.27-fold. Figures 3.9D and 3.9E show an increase at the *PLK1* promoter site by 1.26-fold and at the *CDK1* promoter site by 1.35-fold. At the *CCNB1* promoter site there was a 1.52-fold increase in *RBL2* enrichment (Figure 3.9F). These were not statistically significant.

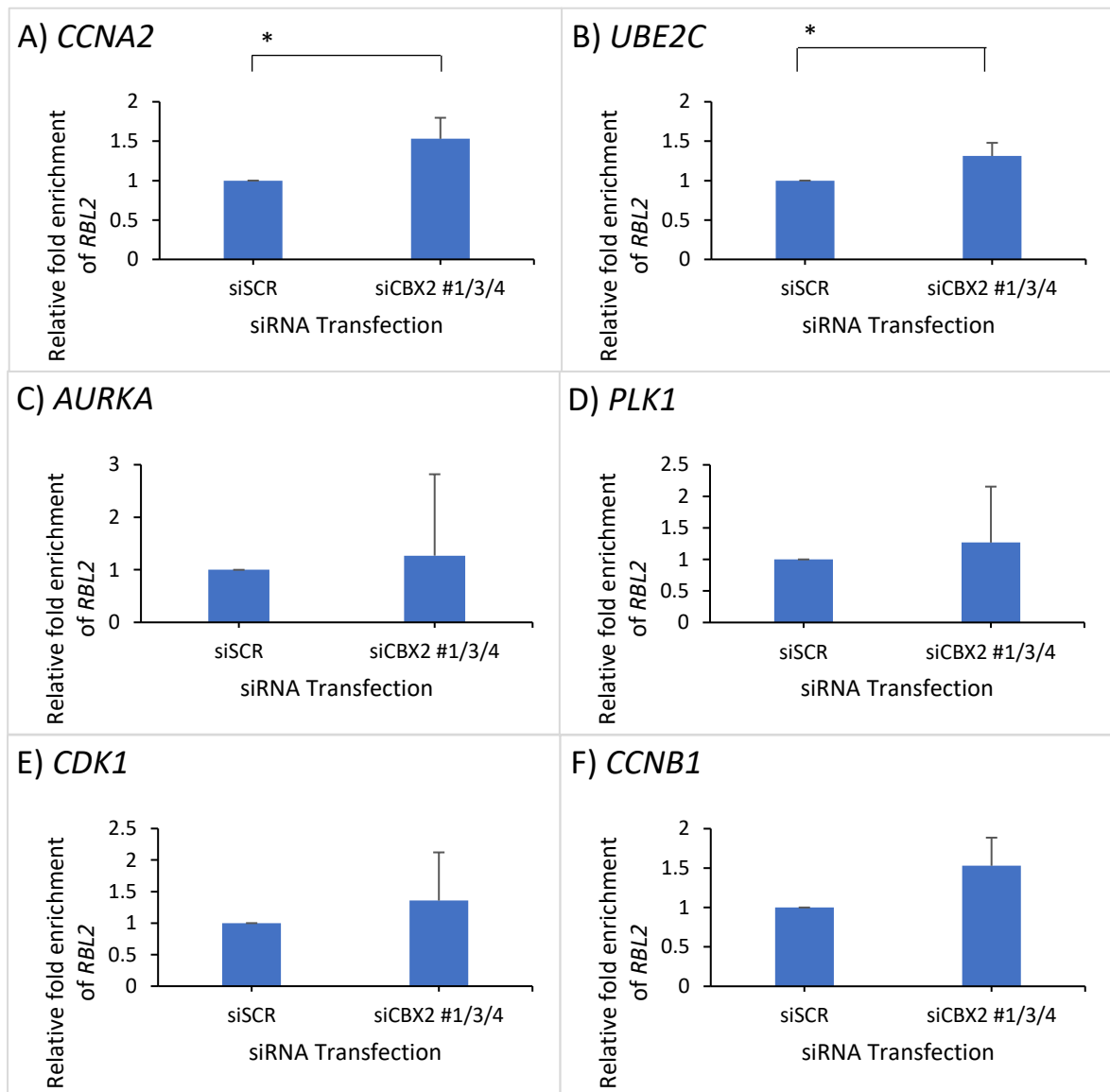


Figure 3.9 Relative fold enrichment of RBL2 at RBL2 promoter sites in MDA-MB-468 cells

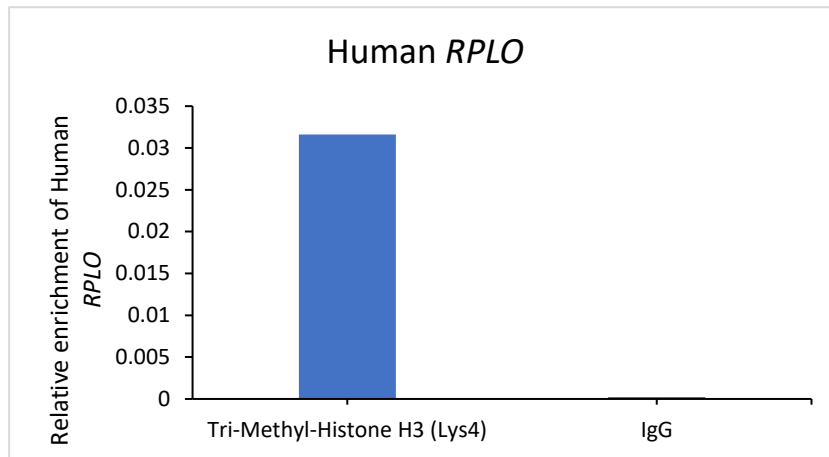
MDA-MB-468 cells were transfected with either an siRNA pool of siCBX2 #1/3/4 or a non-silencing control siRNA (siSCR). 2 million cells were plated onto a large dish and the cells were grown for 72 hours. After incubation, a ChIP was carried out using an anti-RBL2 antibody. Enrichment was calculated as percentage input and made relative to the percentage input in siSCR transfected cells. Error bars represent standard deviation. A Student's T test was carried out. *CCNB1*, *UBE2C* n=3. *AURKA*, *PLK1*, *CCNA2*, *CDK1* n=4.

### 3.8 Determining CBX2 chromatin interactions via CUT & RUN sequencing

To understand the role CBX2 has in the regulation of gene expression in TNBC, it is important to understand where CBX2 is binding on the chromatin and therefore which genes it may be directly regulating. ChIP-sequencing has been widely used for this type of analysis however recently new technologies have been developed for genome-wide chromatin binding studies. One such technique is called CUT & RUN which works by conjugating an MNase protein to an antibody bound to the target protein which then digests the DNA either side of the protein of interest (Skene & Henikoff, 2017). This technique can be done on far fewer cells than ChIP-sequencing (100,000 compared to millions of cells), has reduced sequencing background noise compared with ChIP-sequencing and does not require the sequencing depth that ChIP-sequencing does; meaning it could be a potentially more precise and cheaper technique to use. CUT & RUN-sequencing has not been done for CBX2 yet so two different CBX2 antibodies were used alongside a positive control antibody (H3K4me3) to test if this was possible.

First a CUT & RUN was carried out using the H3K4me3 antibody as a positive control and an IgG as a negative control to determine if the protocol worked. qPCR analysis was used to analyse the enrichment of these two controls on the Human *RPL0* gene. *RPL0* is constitutively expressed and H3K4me3 is a marker for transcriptional activation. Figure 3.10A shows enrichment of H3K4me3 at the *RPL0* promoter and essentially no enrichment when using the IgG antibody, thus indicating that the CUT & RUN technique worked. After this experiment a CUT & RUN was carried out on MDA-MB-231 cells using two anti-CBX2 antibodies (Abcam and Diagenode), an IgG and the H3K4me3 positive control antibody (N=2). Before the samples were sent for sequencing a qPCR analysis was used to see if the protocol worked and if there was enrichment of positive and negative controls on the Human *RPL0* gene. Figure 3.10B shows the first (n=1) and second (n=2) repeats. The figure shows higher enrichment in the H3K4me3 marker and low enrichment in the negative control showing that the CUT & RUN technique worked however, it cannot be confirmed that the two anti-CBX2 antibodies worked as they have not been validated for CUT & RUN. The samples were sent to Novogene for sequencing. At the time of writing this thesis only the preliminary QC data had returned for this experiment, which is detailed below.

A)



B)

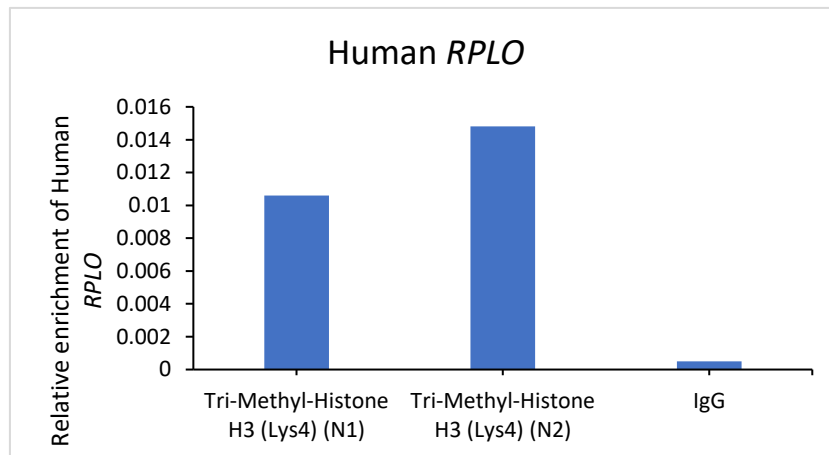


Figure 3.10 CUT & RUN on MDA-MB-231 cells

MDA-MB-231 cells were harvested, and a CUT & RUN was carried out using the Tri-Methyl-Histone H3 (Lys4) antibody as a positive control and an IgG as a negative control. Enrichment at the promoter of *RPLO* was assessed by qPCR. (A) Initial assessment of the CUT & RUN protocol. (B) Validation of the CUT & RUN protocol worked for samples to be sent for sequencing. The data was normalised by normalising the raw data to one sample and then using this data to normalise the percentage inputs of the samples. Figure B shows raw percentage input.

### 3.8.1 Quality Control analysis of Cut & Run-sequencing

It was shown from the initial QC analysis that both CUT & RUN experiments had produced very low amounts (0.1-0.2 ng/ $\mu$ l) of DNA for sequencing. Low amounts of DNA are expected from CUT & RUN experiments due to the low input of starting material being used and then during the protocol the DNA is further reduced during the immunoprecipitation. The input sample had a higher concentration of DNA (10.5 ng/ $\mu$ l), this is due to not going through the immunoprecipitation part of the protocol. The NEBNext® Ultra™ IIDNA Library Prep Kit (a specific low input method of library preparation) was used due to the low levels of DNA. The sequencing for each sample was successful and the data quality summary can be seen in Table 3.1.

*Table 3.1 Data quality summary of CUT & RUN sequencing. “Sample” indicates what the target protein was, and which antibody was used (Abcam or Diagenode for CBX2) as well as which biological repeat this DNA was from (n=1 or n=2). The sequencing was done in two batches. Which sample was in which batch is indicated by the red and blue shading*

<b>Sample</b>	<b>Raw Reads</b>	<b>Clean Reads (%)</b>	<b>Error (%)</b>	<b>GC Content (%)</b>
CBX2 Abcam n=1	43708190	63.87	0.03	52.27
CBX2 Abcam n=2	45597240	81.5	0.03	47.44
CBX2 Diagenode n=1	53569508	69.11	0.03	52.52
CBX2 Diagenode n=2	46496618	74.69	0.03	53.22
H3K4me3 n=1	43751584	73.27	0.03	53.22
H3K4me3 n=2	45635146	92.21	0.03	55.32
Input	47161064	97.88	0.03	42.2

Sample: Sample name.

Raw reads: total amount of reads of raw data.

Clean Read (%): (Number of clean reads/Raw reads)\*100%

Error (%): base error rate

GC Content (%): (G and C base count/Total base count)\*100%

The results show that the sequencing was successful and error free as the percentage error rate for all samples was low (0.3%). The GC content of sequence produced should be around 50%, which was true of all samples. The input sample had a lower GC Content percentage (42.2%), but this was still within QC parameters. The sequenced reads (raw reads) can contain low quality reads and reads that contain sequencing adapters. To determine the percentage of “clean reads” containing genomic sequence that can confidently be mapped to the genome, the raw reads are filtered to remove those containing adapters and those containing >10% of reads in which the base could not be determined. For each sample, the

reads only contained clean reads or adapter related reads. The samples were sequenced in two different batches by Novogene, which is shown by the blue and red shaded samples in the table. The results show that the percentage of clean reads was higher in all samples from the first run (81.5%-97.88% - blue shaded samples) compared to the second run (63.87%-73.27% - red shaded samples). This may be due to chance or technical differences within each sequencing run.

In summary each CUT& RUN experiment produced DNA, from which a successful library was generated that was able to be sequenced. To determine if the CUT & RUN itself worked the sequence will be mapped to the genome and the areas mapped assessed to identify regions that CBX2 binds to and that the H3K4me3 mark is deposited. This analysis was not complete at the time of writing.

## Chapter 4 Discussion

TNBC is very difficult to treat, partly due to the lack of ER, PR and HER2 receptors present, meaning they cannot be treated with targeted endocrine therapy. Due to this, patients with this aggressive subtype of breast cancer tend to have a poor prognosis. Therefore, it is critical that new novel therapeutic options are identified to treat patients diagnosed with TNBC. CBX2 is an epigenetic protein found to play a role in cancer and studies have shown it to be upregulated in many cancers such as lung, colon, stomach, and breast (Clermont et al, 2014). Liang et al, 2017 also confirmed via analysis of publicly available patient gene expression databases that *CBX2* was expressed in breast cancer and that it was higher compared to normal breast samples. The overexpression of *CBX2* was also more prominent in TNBC compared to other breast cancer subtypes.

The aim of this study was to investigate the role of CBX2 in TNBC cell growth. In this project we have confirmed that CBX2 knockdown reduces the growth of TNBC cells. After CBX2 knockdown the tumour suppressor protein RBL2 was upregulated and the expression of RBL2 target genes was reduced. RBL2 is a member of the DREAM complex, which inhibits the cell cycle via preparation of cell cycle gene expression. We observed that following CBX2 knockdown RBL2 enrichment at a subset of DREAM complex target sites was elevated. In addition, a cutting edge CUT&RUN protocol to determine CBX2 binding sites was optimised, and samples sent for sequencing.

### 4.1 CBX2 knockdown causes reduced cell growth

To investigate the role CBX2 has on cell growth, a transfection was carried out on MDA-MB-468 cells using either siSCR or siCBX2 #1/3/4. Cells were grown for 96 hours before they were trypsinised and counted. It has previously been seen in MDA-MB-231 cells that CBX2 knockdown caused a reduction in cell growth, so another TNBC cell line was used to see if these effects could be repeated. All three siCBX2 conditions showed a statistically significant reduction in cell growth compared to the scrambled control, with siCBX2 #4 showing the most reduction.

To further validate the effects observed from the cell count results, an SRB assay was carried out on the same cell line. All three siCBX2 conditions did show a reduced absorbance compared to the siSCR thus showing a reduction in cell growth, however, these results were not statistically significant.

Differences are likely to be observed between the two tests used as manual cell counts measure the total number of cells present whereas an SRB assay measures the amount of protein content that has been stained with SRB. There are also limitations to both assays that can affect the results seen. For example, with manual cell counts there is the potential for user bias as the cell count number would vary from person to person as well as due to the cell suspension being loaded into a chamber on a haemocytometer there is the chance of uneven distribution of the cells. These two points can lead to the overestimation or underestimation of the how many cells are present affecting the results (Johnston, 2010). A crucial step that can affect the outcome of results of an SRB assay is the multiple washing steps. If the wash steps are too harsh there is the risk of cells becoming dislodged from the plate or if the washing is not sufficient there can be excess dye still bound to the cells which can give an inaccurate result (Vichai & Kirtikara, 2006).

Reduced cell growth in other breast cancer cell lines has been observed. CBX2 was knocked down in the oestrogen receptor positive cell line MCF-7 and the TNBC cell line MDA-MB-231 (Zheng et al, 2019). Cells from both cell lines were counted after incubation and both showed reduced proliferation which suggests CBX2 plays a role in cell growth in breast cancer (Zheng et al, 2019). When comparing the Zheng et al, 2019 study which used short hairpin RNA (shRNA) targeting CBX2 via lentiviral transduction of a plasmid to ours, we used 3 independent siRNA sequences which is arguably a more robust way of determining the effect of CBX2 on cell growth. It can be concluded from this data that CBX2 is required for TNBC cell growth thus targeting CBX2 could be useful.

#### 4.2 RBL2 expression is upregulated after the knockdown of CBX2 and there is no effect on E2F4

Previous RNA-sequencing analysis in the Wade lab identified that knockdown of CBX2 in the TNBC cell line MDA-MB-231, increased the expression of the tumour suppressor gene *RBL2*. To look at the effect of CBX2 knockdown at the protein level in MDA-MB-231 and MDA-MB-468 cells, RBL2 expression was analysed through western blot. Both cell lines were transfected with siSCR and siCBX2 #1/3/4. Western blot analysis showed that following CBX2 knockdown the expression of RBL2 increased in both TNBC cell lines. This suggests that CBX2 represses RBL2 and when CBX2 is knocked down, the expression of RBL2 is upregulated. RBL2 is part of the DREAM complex with E2F4 and plays a role in preventing progression of cells through the cell cycle. De-regulation of RBL2 has been observed in different cancers such as oral squamous carcinoma, uveal melanoma and endometrial

carcinoma (Ullah et al, 2015). It has also been reported that loss of RBL2 in the early stages of breast cancer, ovarian cancer, endometrial cancer and non-small lung cancer can be used as an important marker of cancer progression (Ullah et al, 2015). Inhibition of RBL2 by CBX2 may therefore be a mechanism by which CBX2 promotes cancer progression

#### 4.3 Formation of DREAM complex after CBX2 knockdown

Due to increased RBL2 expression after CBX2 knockdown, co-IP for another DREAM complex component, E2F4, was carried out to determine whether this increased expression would show increased formation of the DREAM complex. E2F4 expression was shown not to be affected by CBX2 knockdown in our experiments, so any increase in interaction between RBL2 and E2F4 would suggest that the increase in RBL2 expression was instigating DREAM complex formation. MDA-MB-468 cells were transfected with either siSCR or siCBX2 #3 and grown for 72 hours. After incubation two separate co-IPs were carried out, one using an anti-RBL2 antibody and the other using an anti-E2F4 antibody. Western blot analysis was carried out to visualise the IPs. The RBL2 IP showed an RBL2 band at 110 kDa in the siCBX2 cells and the siSCR cells. However, no band was seen for E2F4 in both the siSCR cells and the siCBX2 cells. It is unclear therefore whether the E2F4 IP worked as no band was detected for E2F4 however, a band was detected for RBL2 which was more intense in the siCBX2 cells following E2F4 IP. It is therefore inconclusive whether the E2F4 IP worked as no E2F4 was detected thus making it hard to confirm whether there is an increase in the formation of the DREAM complex.

Due to not being able to confirm whether the E2F4 IP was successful or not it is likely that the IP protocol needs trouble shooting and optimising. A key component of the co-IP protocol that can affect the outcome of the experiment is the lysis buffer used. A lysis buffer used that is too harsh due to high salt concentrations and an incorrect pH can alter protein interactions, reduce antibody binding and overall denature the proteins being investigated (DeCaprio & Kohl, 2020). A possible step to carry out would be to reduce the salt concentrations by using a lower concentration of NaCl, adding in non-ionic detergents such as NP40 or titron-X 100 and to adjust the pH. Research shows an optimal pH range of lysis buffer is 6-9 (DeCaprio & Kohl, 2020). The previous lysis buffer used, and new optimised buffer could be used as controls in a co-IP to see the outcome of the different buffers. It is also essential an IgG negative control is used to confirm that binding of protein in the other samples are from the specific protein of interest (Lagundžin et al., 2022). Furthermore, the input samples should also be included as these samples confirm if there is protein present.

#### 4.4 CBX2 knockdown increases gene expression of *RBL2* and affects *RBL2* target genes

Gene expression profiling was carried out on MDA-MB-468 cells to see if *RBL2* expression was affected and if this also affected *RBL2* target genes. MDA-MB-468 cells were transfected with siSCR or siCBX2 #1/#3/#4 and grown for 72 hours. After incubation an RNA extraction and reverse transcription was carried out to generate cDNA. The samples were then analysed through qPCR and the primers for the following genes were analysed: *CBX2*, *RBL2*, *PLK1*, *AURKA*, *CCNA2* and *CDK1*. For the analysis of *PLK1*, *AURKA*, *CCNA2* and *CDK1*. siCBX2 #1 was not used it was agreed that this siRNA was not as effective compared to siCBX2 #3 and #4 for CBX2 knockdown. Following knockdown of *CBX2*, *RBL2* expression was increased in siCBX2 #1 and #3 conditions however siCBX2 #4 showed a decrease in expression, which was unexpected. Each siCBX2 condition was statistically significant. It was seen in all repeats for the analysis of *RBL2* that siCBX2 #4 was decreased which contradicts previous RNA-sequencing data in MDA-MB-231 cells and the western blots results which showed increased *RBL2*. The results observed for siCBX2 #4 may be due to issues with the qPCR, although this cannot be explained at this time. *RBL2* target genes repressed by the DREAM complex all showed a decreased in each siCBX2 condition apart from *CDK1* which showed no change. Results for siCBX2 #3 and #4 for *PLK1* and *CCNA2* were statistically significant.

*PLK1*, *AURKA*, *CCNA2* AND *CDK1* all play important roles in the regulation of the cell cycle. *PLK1* and *AURKA* are both kinases. *PLK1* is involved in mitosis through mechanisms such as spindle assembly, centrosome maturation, sister chromatid cohesion and recovery from DNA-damage induced rest. *AURKA* is involved in spindle formation in mitosis by phosphorylating *PLK1* (Bruinsma et al, 2015). *CDK1* is a cyclin-dependent kinase that regulates the cell cycle from the entry of cells through to S phase and is involved in mitosis. *CCNA2* binds to *CDK1*, and this complex helps cells progress through the S phase of the cell cycle (Diril et al, 2012; Li et al, 2021). These genes are essential in the cell cycle and downregulation of these genes would result in cells being unable to progress through the cell cycle and would therefore reduce cell growth and cause cell senescence. When cells are in senescence, senescence-associated  $\beta$ -galactosidase (SA- $\beta$ -Gal) activity is increased thus, using this staining technique can aid in differentiating normal and senescent cells (González-Gualda et al., 2021).

#### 4.5 CBX2 knockdown increases *RBL2* enrichment at DREAM complex target sites

To further investigate the effect of CBX2 knockdown on *RBL2* and DREAM complex activity, the enrichment of *RBL2* at DREAM complex target sites was investigated by ChIP. MDA-MB-231 and MDA-MB-468 cells were transfected with either siSCR or an siRNA

pool of siCBX2 #1/3/4 and after incubation ChIPs were carried out using an anti-RBL2 antibody. qPCR analysis showed that in MDA-MB-231 cells following the knockdown of CBX2, RBL2 was enriched at the promoter sites of *CCNA2*, *CCNB1*, *PLK1*, *AURKA* and there was no change at the promoter sites of *CDK1*, *UBE2C* and *UBE2S*. RBL2 enrichment was decreased at the *CDC20* promoter site. *CCNA2*, *CDC20* and *CCNB1* were statistically significant. In MDA-MB-468 cells after CBX2 knockdown RBL2 was enriched at the promoter sites of *CCNA2*, *UBE2C*, *AURKA*, *PLK1*, *CDK1* and *CCNB1*. *CCNA2* and *UBE2C* were statistically significant.

The increased enrichment of RBL2 at DREAM complex sites suggests that following CBX2 knockdown there is an increase in DREAM complex formation at these genes. The DREAM complex is important in regulating the cell cycle by halting the process of cancerous cells leading to cell senescence (Gaubatz et al, 2000). Due to CBX2 inhibiting RBL2 and the DREAM complex this opens the potential for CBX2 to be therapeutically targeted in order to reactivate DREAM complex activity to and slow cancer growth. To provide further evidence to support the hypothesis that there is dysregulated DREAM complex recruitment more ChIP assays could be carried out. Different components of the DREAM complex such as E2F4, DP and MuvB could be analysed to identify if there is any enrichment following CBX2 knockdown. qPCR analysis could be carried out with the same genes used prior to identify if there is increased enrichment of the DREAM components at these sites.

Recently, SW2\_152F a selective CBX2 inhibitor has been developed that blocks the CBX2 chromodomain to prevent chromatin binding and PRC1 complex formation. Using DNA encoded libraries, molecules were generated which showed an increased level of affinity ( $K_d$  80nM) and selectivity of 24 to 1000-fold to CBX2 compared to other CBX orthologues. To confirm the effects of SW2\_152F, a prostate cancer cell line LNCaP\_NED was treated with the inhibitor. Inhibitor treatment reduced cell proliferation and decreased cell size (Wang et al, 2021). The inhibitor also reduced CBX2 enrichment and CBX2 target genes showing that the inhibitor prevents the chromatin binding of CBX2. Thus, the data generated by this paper shows the proof of principle that CBX2 inhibitors could be created which in the future could potentially be used for the treatment of TNBC.

Furthermore, there are other inhibitors that target the bromodomain and extraterminal domain (BET) protein family. BET proteins are responsible for recognising acetylation of lysine residues on histones (Shorstova et al, 2021). In this family there are four main proteins called

BRD2, BRD3, BRD4 and testis-specific BRDT which all share the same structure of two-N-terminal bromodomains (BD) known as BD1 and BD2 (Andrikopoulou et al, 2020). It has been found that the BET proteins can alter the cell cycle progression through the activation of different oncogenes such as *CCNA1*, *MYC*, *CCND1* and *JUNB*. This process arises through BET proteins acting as a scaffold to super enhancers which are areas of the genome which have multiple enhancers bound by TFs and coactivators that known to initiate expression of oncogenes and disease associated genes. (Andrikopoulou et al, 2020; Shorstova et al, 2021). BRD4 also interacts with positive transcription elongation factor (PTEF-b), recruiting it to sites of active transcription. PTEF-b is then activated by the phosphorylation of the CDK9 component in the protein which ultimately leads to the phosphorylation of RNA Polymerase II initiating transcription (Andrikopoulou et al, 2020). JQ1 was developed to inhibit BRD4. It works by mimicking the acetylated lysine residue enabling it to bind to the binding pockets of BRD4 which prevents other proteins being recruited to the chromatin site halting transcription and induces cell cycle arrest (Shorstova et al, 2021). Treatment of JQ1 in TNBC cell lines resulted in cell cycle arrest in the G1 phase (Andrikopoulou et al, 2020).

#### 4.6 CUT & RUN to further understand CBX2 chromatin interactions on the genome

A CUT & RUN-sequencing experiment was carried out to help identify where CBX2 binds on the chromatin, and thus, what genes it may regulate the expression of. To determine if the process works the first CUT & RUN carried out was on MDA-MB-231 cells using a positive (H3K4me3) and IgG negative control. qPCR analysis was carried out using the Human *RPL0* gene which showed that there was enrichment of H3K4me3 and low enrichment of the IgG, confirming that the process worked. After a successful first experiment a second CUT & RUN was carried out using two different CBX2 antibodies as well as the H3K4me3 control and IgG control. A qPCR analysis using the positive and negative control and the Human *RPL0* gene was analysed. This identified that the process worked as there was higher enrichment of H3K4me3 and low enrichment of the IgG. These samples were then sent to Novogene for sequencing. The initial sequencing results showed that the samples contained low amounts of DNA and the input sample had a higher quantity of DNA, both results are expected from CUT & RUN. NEBNext® Ultra™ IIDNA Library Prep Kit was used due to the low levels of DNA and generated a successful library that can be sequenced. It was identified that both repeats of the CUT & RUN experiment were successful and error free. The next step that could not be completed due to time constraints would be for the sequence

to be mapped to the genome and the areas mapped assessed to identify regions that CBX2 binds to and that the H3K4me3 mark is deposited.

Before the CUT & RUN protocol was developed ChIP was predominately used to identify where proteins are bound along the chromatin. Although this is still widely used there are also some disadvantages to the ChIP protocol which led to the development of CUT & RUN to resolve these problems. ChIP often requires millions of cells at a time to carry out the protocol which may not always be readily available. CUT & RUN is optimised to use a far lower cell number, a minimum of 100,000 cells per reaction, which means it is applicable to samples where cell numbers are limited such as patient tumour tissue (Hainer & Fazzio, 2019). During the ChIP protocol there is a sonication step which solubilises the whole of the chromatin rather than just the area that is being investigated. This then leads to the need of very deep sequencing of the genome which is expensive and often results in high background noise (Skene & Henikoff, 2017). CUT & RUN minimises this problem by adding an antibody and pAG-MNase to unfixed cells/nuclei. The MNase component is activated through the addition of calcium and the cells are not damaged. This then allows for the chromatin to be cleaved only around the area of the target sites on the chromatin and released into a solution rather than the whole genome being solubilised. Due to the smaller sample of chromatin this reduces the sequencing depth by ~10 fold thus lowering the cost of sequencing and ultimately giving a higher quality genome profile and reduced background noise (Meers et al, 2019). Using the CUT & RUN protocol to help identify where CBX2 is bound on the genome would be beneficial in further understanding what genes are being targeted.

There are also disadvantages with the CUT & RUN protocol. There is the issue of not all antibodies working and only a limited amount of antibodies are CUT & RUN validated. This limits the range of proteins that can be analysed until more antibodies are validated (Cell Signaling Technology, 2023). The protocol is technically challenging thus the need for optimisation of steps for the best outcome of results. Although the amount of digitonin recommended in the protocol is likely to be sufficient to permeabilise the cells, some cells and tissues are difficult to permeabilise so there is the risk of some cells/tissues not being appropriate to use for the protocol if optimisation is not successful (Cell Signaling Technology, 2023). As seen in the protocol there are many steps involved with different incubation times, any variability in these steps could cause inconsistent results. Despite the advantage of the chromatin sample being smaller once cleaved by MNase, there are

modifications that need to be made for applications such as library preparation (Cell Signaling Technology, 2023).

#### 4.7 Conclusion

The main findings of this study are that CBX2 promotes cell growth in TNBC. Figure 4.1 shows that CBX2, as part of the PRC1 complex, targets and suppresses *RBL2* expression. Suppression of the *RBL2* gene leads to less RBL2 protein which ultimately results in reduced formation of the DREAM complex. When there is less DREAM complex formation this allows the cell cycle to become unregulated and causes cells to proliferate. It also can be seen in figure 4.1 the alternate route when CBX2 is inhibited. Inhibition of CBX2 would increase *RBL2* gene expression and RBL2 protein expression which in turn may initiate the formation of the DREAM complex. Upregulation of DREAM complex formation would allow for regulation of the cell cycle through repression of specific cell cycle genes which may prevent cancerous cells from proliferating, thereby reducing cell growth.

It is currently unknown whether H3K27me3 is present at the *RBL2* promoter. CBX2 ChIP-sequencing of A549 cells, which are a lung adenocarcinoma cell line, showed that 6.4% of CBX2 binding sites overlapped with regions containing H3K27me3, whereas only 0.2% of H3K27me3 binding sites overlapped with the CBX2 binding sites. This suggests that CBX2 associated PRC1 can bind independently of H3K27me3. This is further supported by the finding that in certain pathways CBX2 and EZH2 (part of PRC2 which deposits methylation on H3K27) were bound to different target genes (Hu et al, 2022). Conversely, ChIP-qPCR assays have shown that at specific target genes, such as *CLDN11*, CBX2 knockdown decreased H2AK119ub as well as decreasing H3K27me3. This shows that the presence of H3K27me3 may be influenced by the absence of presence of CBX2 (Hu et al, 2022). Analysis of the presence of H3K27me3 at the *RBL2* promoter would need to be done in order to understand the interaction between CBX2 and H3K27me3 to control *RBL2* expression.

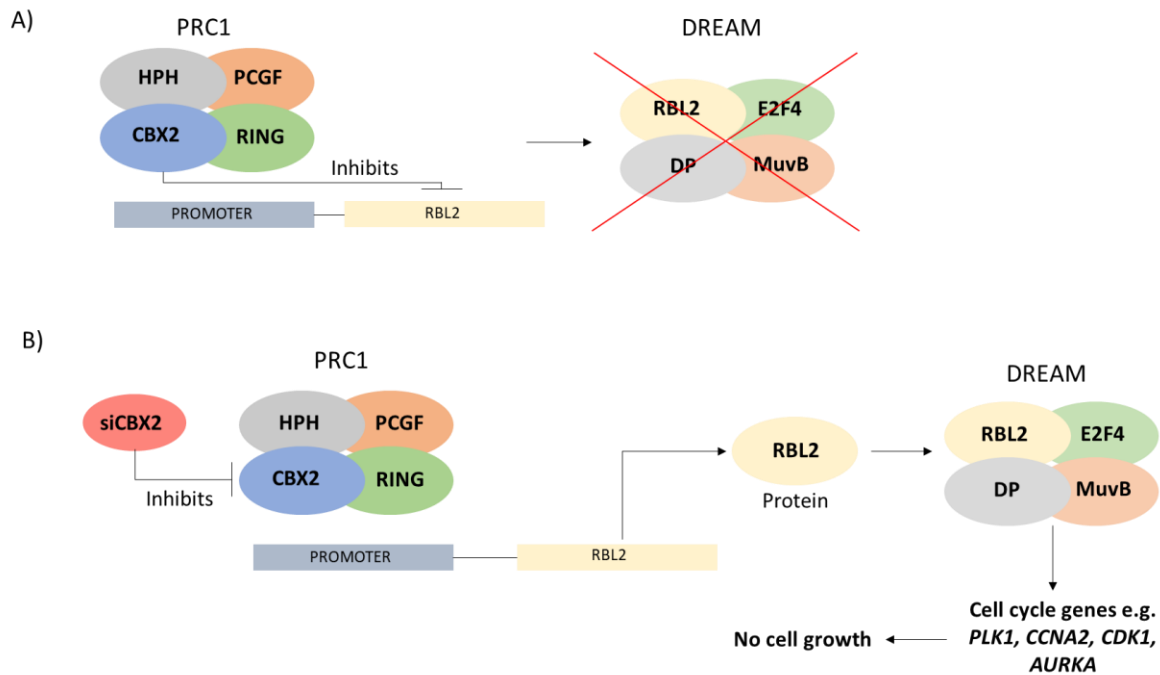


Figure 4.1 Effect of CBX2 suppressing RBL2

A) CBX2 as part of PRC1 inhibits *RBL2* expression causing reduced DREAM complex formation. B) When CBX2 is inhibited *RBL2* expression is increased and there is increased formation of the DREAM complex which inhibits cycle genes thereby preventing progression through the cell cycle and limiting cell growth.

## Future Directions

The next steps for this study would be to carry out further analysis on the CUT & RUN sequencing to identify the areas that CBX2 is bound to. The group already have RNA-sequencing data of genes differentially regulated following CBX2 knockdown. Combining CUT & RUN data with differentially expressed gene lists may indicate which genes CBX2 is directly regulating, and which genes are differentially expressed due to downstream signalling. This would be done by cross referencing genes from RNA-sequencing data that are differentially expressed after CBX2 knockdown with genes that CBX2 is bound to the promoters of. Additionally, acquiring ChIP-sequencing data for the RBL2 ChIP samples would help give further insight into areas on the genome RBL2 is interacting with and which target genes are affected by CBX2 mediated downregulation of RBL2.

The use of PDX models in helping validate CBX2 as a therapeutic target would also be beneficial. This could be done by cross referencing CBX2 CUT & RUN-sequencing and/or ChIP-sequencing analysis in PDX samples with MDA-MB-231 cells or other to TNBC cell lines to compare binding sites. This would help to provide translationally relevant validation for the binding sites identified in cell lines and help determine whether CBX2 regulates similar genes in patient tissue.

Another useful step would be to compare the effect of CBX2 knockdown with the treatment of the novel inhibitor developed by Wang et al (2021). Methods such as cell growth assays, cell cycle assays (flow cytometry), gene expression analysis of *RBL2* as well as other CBX2 regulated genes or RNA-sequencing, could be carried out in SW2\_152F treated cells to analyse the effects of the inhibitor in TNBC cell lines. As well as this, carrying out ChIP-qPCR of SW2\_152F treated cells to see if this blocks CBX2 from binding at identified CBX2 binding sites would help validate the peptide as a true CBX2 specific chromodomain inhibitor. Carrying out these methods will help strengthen validation of the specificity of the CBX2 inhibitor and it would cross validate the CBX2 knockdown analysis. Another step to head towards would be to use SW2\_152F *in vivo* mouse cell line xenografts or PDX xenografts to assess the effect of CBX2 inhibition in a more translationally relevant model.

These steps discussed would further validate the findings of this study along with helping to assess the utility of the CBX2 inhibitor in preventing TNBC growth, ultimately adding translational validation that CBX2 is a genuine therapeutic target for TNBC.

## References

Abcam.com. 2022. *SRB Assay / Sulforhodamine B Assay Kit (ab235935) | Abcam*. [online] Available at: <<https://www.abcam.com/SRB-Assay--Sulforhodamine-B-Assay-Kit-ab235935.html>>

Abdelraheem, E. M. M., Thair, B., Varela, R. F., Jockmann, E., Popadić, D., Hailes, H. C., Ward, J. M., Hagedoorn, P. L. & Hanefeld, U. (2022) Methyltransferases: Functions and applications. *Chembiochem : A European Journal of Chemical Biology*, 23 (18), e202200212-n/a.

Akram, M., Iqbal, M., Daniyal, M. and Khan, A., 2017. Awareness and current knowledge of breast cancer. *Biological Research*, 50(1).

Alves-Fernandes, D. K. & Jasiulionis, M. G. (2019) The role of SIRT1 on DNA damage response and epigenetic alterations in cancer. *International Journal of Molecular Sciences*, 20 (13), 3153.

Andrikopoulou, A., Lontos, M., Koutsoukos, K., Dimopoulos, M. & Zagouri, F. (2020) The emerging role of BET inhibitors in breast cancer. *Breast (Edinburgh)*, 53 152-163.

Audia, J. E. & Campbell, R. M. (2016) Histone modifications and cancer. *Cold Spring Harbor Perspectives in Biology*, 8 (4), a019521.

Bannister, A. J. & Kouzarides, T. (2011) Regulation of chromatin by histone modifications. *Cell Research*, 21 (3), 381-395.

Bielski, C. M. & Taylor, B. S. (2021) Homing in on genomic instability as a therapeutic target in cancer. *Nature Communications*, 12 (1), 3663.

Bilton, L. J., Warren, C., Humphries, R. M., Kalsi, S., Waters, E., Francis, T., Dobrowinski, W., Beltran-Alvarez, P. & Wade, M. A. (2022) The epigenetic regulatory protein CBX2 promotes mTORC1 signalling and inhibits DREAM complex activity to drive breast cancer cell growth. *Cancers*, 14 (14), 3491.

Biswas, S. & Rao, C. M. (2018) Epigenetic tools (the writers, the readers and the erasers) and their implications in cancer therapy. *European Journal of Pharmacology*, 837 8-24.

Bjoernstroem, L. & Sjoeborg, M. (2005) Mechanisms of estrogen receptor signaling: Convergence of genomic and nongenomic actions on target genes. *Molecular Endocrinology (Baltimore, Md.)*, 19 (4), 833-842.

Bruinsma, W., Aprelia, M., Kool, J., Macurek, L., Lindqvist, A. and Medema, R., 2015. Spatial Separation of Plk1 Phosphorylation and Activity. *Frontiers in Oncology*, 5.

Botstein, D., Perou, C. M., Sørlie, T., Eisen, M. B., van de Rijn, M., Jeffrey, S. S., Rees, C. A., Pollack, J. R., Ross, D. T., Johnsen, H., Akslen, L. A., Fluge, Ø, Pergamenschikov, A., Williams, C., Zhu, S. X., Lønning, P. E., Børresen-Dale, A. & Brown, P. O. (2000) Molecular portraits of human breast tumours. *Nature (London)*, 406 (6797), 747-752.

Cancer Research UK. 2022. *Cancer Statistics for the UK*. [online] Available at: <<https://www.cancerresearchuk.org/health-professional/cancer-statistics-for-the-uk#heading-Zero>>

Cancer Research UK. 2022. *What is cancer?*. [online] Available at: <<https://www.cancerresearchuk.org/about-cancer/what-is-cancer>>

Carroll, J. S. (2016) Mechanisms of oestrogen receptor (ER) gene regulation in breast cancer. *European Journal of Endocrinology*, 175 (1), R41-R49.

Cell Signaling Technology. 2022. *CUT&RUN Overview | Cell Signaling Technology*. [online] Available at: <<https://www.cellsignal.co.uk/applications/cut-and-run-overview>>

Cell Signaling Technology. 2023. *Cut&run Troubleshooting Guide*. [online] Available at: <https://www.cellsignal.com/learn-and-support/troubleshooting/cutandruntroubleshooting-guide>.

Cescon, D. W., Nowecki, Z., Gallardo, C., Holgado, E., Iwata, H., Masuda, N., Otero, M. T., Loi, S., Guo, Z., Gonzalo, G. A., Diego, K., Matias, M., Stephen, B., Philip, C., Sherene, L., Dhanusha, S., Donatienne, T., Domicio Carvalho, L., Fernando Cezar Toniuzzi, L., Felipe, S., Joanne, Y., Alejandro, A., Bohuslav, M., Katarina, P., Jana, P., Erik, J., Jeanette, J., Soren, L., Tamas, L., Herve, B., Isabelle, D., Jens-Uwe, B., Nadia, H., Jens, H., Christian, K., Sibylle, L., Tibor, C., Zsuzsanna, K., Karoly, M., John, C., Seamus, O., Takaaki, F., Hiroji, I., Hirofumi, M., Seigo, N., Shoichiro, O., Akihiko, O., Yasuaki, S., Masato, T., Koichiro, T., Junichiro, W., Yutaka, Y., Teruo, Y., Angel, G. V., Alejandro, J. R., Flavia, M., David, P., Ewa, C., Ewa, N., Zbigniew, N., Barbara, R., Joanna, S., Alexander, A., Natalia, F., Oleg, L., Kwong Hwa, P., Yeon Hee, P., Begona, Bermejo de las Heras, Javier, C., Luis, de la Cruz Merino, Jose, G. S., Maria, G., Mei-Ching, L., Chiun-Sheng, H., Cagatay, A., Irfan, C., Erhan, G., Ozgur, O., Sinan, Y., Janine, G., Mark, T., Christopher, T., Duncan, W., Oleksii, K., Olena, K., Alla, N., Olga, P., Dmytro, T., Sibel, B., Madhu, C., Scott, C., William, I., Randa, L., Janice, L., Coral, O., Timothy, P., Michael, S., Robert, S., Michael, S. & Frances, V. (2020) Pembrolizumab plus chemotherapy versus placebo plus chemotherapy for previously untreated locally recurrent inoperable or metastatic triple-negative breast cancer

(KEYNOTE-355): A randomised, placebo-controlled, double-blind, phase 3 clinical trial. *The Lancet (British Edition)*, 396 (10265), 1817-1828.

Chen, A. (2011) PARP inhibitors : its role in treatment of cancer. *Ai Zheng*, 30 (7), 463-471.

Chen, F., Chen, N., Gao, Y., Jia, L., Lyu, Z. & Cui, J. (2021) Clinical progress of PD-1/L1 inhibitors in breast cancer immunotherapy. *Frontiers in Oncology*, 11 724424.

Chittock, E. C., Latwiel, S., Miller, T. C. R. & Müller, C. W. (2017) Molecular architecture of polycomb repressive complexes. *Biochemical Society Transactions*, 45 (1), 193-205.

Clermont, P.-L, Crea, F., Chiang, Y. T., Lin, D., Zhang, A., Wang, J. Z. L., Parolia, A., Wu, R., Xue, H., Wang, Y., Ding, J., Thu, K. L., Lam, W. L., Shah, S. P., Collins, C. C., Wang, Y. & Helgason, C. D. (2016) Identification of the epigenetic reader CBX2 as a potential drug target in advanced prostate cancer. *Clinical Epigenetics*, 8 (16), 16.

Clermont, P. -L, Sun, L., Crea, F., Thu, K. L., Zhang, A., Parolia, A., Lam, W. L. & Helgason, C. D. (2014) Genotranscriptomic meta-analysis of the polycomb gene CBX2 in human cancers: Initial evidence of an oncogenic role. *British Journal of Cancer*, 111 (8), 1663-1672.

Cortesi, L., Rugo, H. S. & Jackisch, C. (2021) An overview of PARP inhibitors for the treatment of breast cancer. *Targeted Oncology*, 16 (3), 255-282.

Curtis, C., Shah, S. P., Chin, S., Turashvili, G., Rueda, O. M., Dunning, M. J., Speed, D., Lynch, A. G., Samarajiwa, S., Yuan, Y., Gräf, S., Ha, G., Haffari, G., Bashashati, A., Russell, R., McKinney, S., METABRIC Group, Langerød, A., Green, A., Provenzano, E., Wishart, G., Pinder, S., Watson, P., Markowitz, F., Murphy, L., Ellis, I., Purushotham, A., Børresen-Dale, A., Brenton, J. D., Tavaré, S., Caldas, C. & Aparicio, S. (2012) The genomic and transcriptomic architecture of 2,000 breast tumours reveals novel subgroups.

da Silva, J. L., Cardoso Nunes, N. C., Izetti, P., de Mesquita, G. G. & de Melo, A. C. (2020) Triple negative breast cancer: A thorough review of biomarkers. *Critical Reviews in Oncology/Hematology*, 145 102855.

Dai, X., Li, T., Bai, Z., Yang, Y., Liu, X., Zhan, J. & Shi, B. (2015) Breast cancer intrinsic subtype classification, clinical use and future trends. *American Journal of Cancer Research*, 5 (10), 2929-2943.

DeCaprio, J. & Kohl, T. O. (2020) Immunoprecipitation. *Cold Spring Harbor Protocols*, 2020 (11), pdb.top098509.

Diril, M., Ratnacaram, C., Padmakumar, V., Du, T., Wasser, M., Coppola, V., Tessarollo, L. and Kaldis, P., 2012. Cyclin-dependent kinase 1 (Cdk1) is essential for cell division and suppression of DNA re-replication but not for liver regeneration. *Proceedings of the National Academy of Sciences*, 109(10), pp.3826-3831.

Elsheikh, S., Green, A., Rakha, E., Powe, D., Ahmed, R., Collins, H., Soria, D., Garibaldi, J., Paish, C., Ammar, A., Grainge, M., Ball, G., Abdelghany, M., Martinez-Pomares, L., Heery, D. and Ellis, I., 2009. Global Histone Modifications in Breast Cancer Correlate with Tumor Phenotypes, Prognostic Factors, and Patient Outcome. *Cancer Research*, 69(9), pp.3802-3809.

Erber, R. & Hartmann, A. (2020) Understanding PD-L1 testing in breast cancer: A practical approach. *Breast Care (Basel, Switzerland)*, 15 (5), 481-490.

Fallah, M., Szarics, D., Robson, C. and Eubanks, J., 2021. Impaired Regulation of Histone Methylation and Acetylation Underlies Specific Neurodevelopmental Disorders. *Frontiers in Genetics*, 11.

Gaubatz, S., Lindeman, G. J., Ishida, S., Jakoi, L., Nevins, J. R., Livingston, D. M. & Rempel, R. E. (2000) E2F4 and E2F5 play an essential role in pocket Protein-Mediated G1 control. *Molecular Cell*, 6 (3), 729-735.

Gahan, J. M., Rentzsch, F. & Schnitzler, C. E. (2020) The genetic basis for PRC1 complex diversity emerged early in animal evolution. *Proceedings of the National Academy of Sciences - PNAS*, 117 (37), 22880-22889.

Gajria, D. & Chandarlapaty, S. (2011) HER2-amplified breast cancer: Mechanisms of trastuzumab resistance and novel targeted therapies. *Expert Review of Anticancer Therapy*, 11 (2), 263-275.

Geng, Z. & Gao, Z. (2020) Mammalian PRC1 complexes: Compositional complexity and diverse molecular mechanisms. *International Journal of Molecular Sciences*, 21 (22), 8594.

Gil, J. & O’Loghlen, A. (2014) PRC1 complex diversity: Where is it taking us? *Trends in Cell Biology*, 24 (11), 632-641.

González-Gualda, E., Baker, A. G., Fruk, L. & Muñoz-Espín, D. (2021) A guide to assessing cellular senescence in vitro and in vivo. *The FEBS Journal*, 288 (1), 56-80.

Greer, E. L. & Yang, S. (2012) Histone methylation: A dynamic mark in health, disease and inheritance. *Nature Reviews. Genetics*, 13 (5), 343-357.

Guo, P., Chen, W., Li, H., Li, M. & Li, L. (2018) The histone acetylation modifications of breast cancer and their therapeutic implications. *Pathology Oncology Research*, 24 (4), 807-813.

Hainer, S. J. & Fazzio, T. G. (2019) High-Resolution chromatin profiling using CUT&RUN. *Current Protocols in Molecular Biology*, 126 (1), e85-n/a.

Hanahan, D. & Weinberg, R. (2011) Hallmarks of cancer: The next generation. *Cell*, 144 (5), 646-674.

Hu, F., Chen, H., Duan, Y., Lan, B., Liu, C., Hu, H., Dong, X., Zhang, Q., Cheng, Y., Liu, M., Guo, A. & Xuan, C. (2022) CBX2 and EZH2 cooperatively promote the growth and metastasis of lung adenocarcinoma. *Molecular Therapy. Nucleic Acids*, 27 670-684.

Hyun, K., Jeon, J., Park, K. & Kim, J. (2017) Writing, erasing and reading histone lysine methylations. *Experimental & Molecular Medicine*, 49 (4), e324.

Iqbal, M. A., Siddiqui, S., Ur Rehman, A., Siddiqui, F. A., Singh, P., Kumar, B. & Saluja, D. (2021) Multiomics integrative analysis reveals antagonistic roles of CBX2 and CBX7 in metabolic reprogramming of breast cancer. *Molecular Oncology*, 15 (5), 1450-1465.

Johnston, G. (2010) Automated handheld instrument improves counting precision across multiple cell lines. *BioTechniques*, 48 (4), 325-327.

Kanwal, R. & Gupta, S. (2012) Epigenetic modifications in cancer. *Clinical Genetics*, 81 (4), 303-311.

Kawaguchi, T., Machida, S., Kurumizaka, H., Tagami, H. & Nakayama, J. (2017) Phosphorylation of CBX2 controls its nucleosome-binding specificity. *Journal of Biochemistry (Tokyo)*, 162 (5), 343-355.

Kent, L. N. & Leone, G. (2019) The broken cycle: E2F dysfunction in cancer. *Nature Reviews. Cancer*, 19 (6), 326-338.

Keung, M. Y. T., Wu, Y. & Vadgama, J. V. (2019) PARP inhibitors as a therapeutic agent for homologous recombination deficiency in breast cancers. *Journal of Clinical Medicine*, 8 (4), 435.

Lagundžin, D., Krieger, K. L., Law, H. C. -. & Woods, N. T. (2022) An optimized co-immunoprecipitation protocol for the analysis of endogenous protein-protein interactions in cell lines using mass spectrometry. *STAR Protocols*, 3 (1), 101234.

Lehmann, B. D., Bauer, J. A., Chen, X., Sanders, M. E., Chakravarthy, A. B., Shyr, Y. & Pietenpol, J. A. (2011) Identification of human triple-negative breast cancer subtypes and preclinical models for selection of targeted therapies. *The Journal of Clinical Investigation*, 121 (7), 2750-2767.

Li, H., Weng, Y., Wang, S., Wang, F., Wang, Y., Kong, P., Zhang, L., Cheng, C., Cui, H., Xu, E., Wei, S., Guo, D., Chen, F., Bi, Y., Meng, Y., Cheng, X. and Cui, Y., 2021. CDCA7 Facilitates Tumor Progression by Directly Regulating CCNA2 Expression in Esophageal Squamous Cell Carcinoma. *Frontiers in Oncology*, 11.

Li, X., Wu, C., Chen, N., Gu, H., Yen, A., Cao, L., Wang, E. & Wang, L. (2016) PI3K/akt/mTOR signaling pathway and targeted therapy for glioblastoma. *Oncotarget*, 7 (22), 33440-33450.

Liang, Y., Lin, H., Chen, C. & Zeng, D. (2017) Prognostic values of distinct CBX family members in breast cancer. *Oncotarget*, 8 (54), 92375-92387.

Litovchick, L., Sadasivam, S., Florens, L., Zhu, X., Swanson, S. K., Velmurugan, S., Chen, R., Washburn, M. P., Liu, X. S. & DeCaprio, J. A. (2007) Evolutionarily conserved multisubunit RBL2/p130 and E2F4 protein complex represses human cell cycle-dependent genes in quiescence. *Molecular Cell*, 26 (4), 539-551.

Liu, Z., Zhang, X. and Zhang, S., 2014. Breast tumor subgroups reveal diverse clinical prognostic power. *Scientific Reports*, 4(1).

Livak, K. J. & Schmittgen, T. D. (2001) Analysis of relative gene expression data using real-time quantitative PCR and the  $2^{-\Delta\Delta CT}$  method. *Methods (San Diego, Calif.)*, 25 (4), 402-408.

Mateo, J., Lord, C. J., Serra, V., Tutt, A., Balmaña, J., Castroviejo-Bermejo, M., Cruz, C., Oaknin, A., Kaye, S. B. & de Bono, J. S. (2019) A decade of clinical development of PARP inhibitors in perspective. *Annals of Oncology*, 30 (9), 1437-1447.

Mao, J., Tian, Y., Wang, C., Jiang, K., Li, R., Yao, Y., Zhang, R., Sun, D., Liang, R., Gao, Z., Wang, Q. & Wang, L. (2019) CBX2 regulates proliferation and apoptosis via the phosphorylation of YAP in hepatocellular carcinoma. *Journal of Cancer*, 10 (12), 2706-2719.

Meers, M. P., Bryson, T. D., Henikoff, J. G. & Henikoff, S. (2019) Improved CUT&RUN chromatin profiling tools. *eLife*, 8 .

Min, A. & Im, S. (2020) Parp inhibitors as therapeutics: Beyond modulation of parylation. *Cancers*, 12 (2), 394.

Nandy, D., Rajam, S. M. & Dutta, D. (2020) A three layered histone epigenetics in breast cancer metastasis. *Cell & Bioscience*, 10 (1), 52.

National Cancer Institute. 2021. *What Is Cancer?*. [online] Available at: <<https://www.cancer.gov/about-cancer/understanding/what-is-cancer>>

Paplomata, E. & O'Regan, R. (2014) *The PI3K/AKT/mTOR pathway in breast cancer: Targets, trials and biomarkers*. London, England: SAGE Publications.

Patel, A., Unni, N. & Peng, Y. (2020) The changing paradigm for the treatment of HER2-positive breast cancer. *Cancers*, 12 (8), 2081.

Rose, M., Burgess, J. T., O'Byrne, K., Richard, D. J. & Bolderson, E. (2020) PARP inhibitors: Clinical relevance, mechanisms of action and tumor resistance. *Frontiers in Cell and Developmental Biology*, 8 564601.

Sadasivam, S. & DeCaprio, J. A. (2013) The DREAM complex: Master coordinator of cell cycle-dependent gene expression. *Nature Reviews. Cancer*, 13 (8), 585-595.

Schütz, F., Stefanovic, S., Mayer, L., von Au, A., Domschke, C. & Sohn, C. (2017) PD-1/PD-L1 pathway in breast cancer. *Oncology Research and Treatment*, 40 (5), 294-297.

Senthilkumar, R. & Mishra, R. K. (2009) Novel motifs distinguish multiple homologues of polycomb in vertebrates: Expansion and diversification of the epigenetic toolkit. *BMC Genomics*, 10 (1), 549.

Shanmugam, M. K., Arfuso, F., Arumugam, S., Chinnathambi, A., Jinsong, B., Warriar, S., Wang, L. Z., Kumar, A. P., Ahn, K. S., Sethi, G. & Lakshmanan, M. (2018) Role of novel histone modifications in cancer. *Oncotarget*, 9 (13), 11414-11426.

Shi, Y., Wang, X., Zhuang, Y., Jiang, Y., Melcher, K. & Xu, H. E. (2017) Structure of the PRC2 complex and application to drug discovery. *Acta Pharmacologica Sinica*, 38 (7), 963-976.

Shorstova, T., Foulkes, W. D. & Witcher, M. (2021) Achieving clinical success with BET inhibitors as anti-cancer agents. *British Journal of Cancer*, 124 (9), 1478-1490.

Skene, P. J. & Henikoff, S. (2017) An efficient targeted nuclease strategy for high-resolution mapping of DNA binding sites. *eLife*, 6 .

Sørlie, T., Perou, C. M., Tibshirani, R., Aas, T., Geisler, S., Johnsen, H., Hastie, T., Eisen, M. B., van de Rijn, M., Jeffrey, S. S., Thorsen, T., Quist, H., Matese, J. C., Brown, P. O., Botstein, D., Lønning, P. E. & Børresen-Dale, A. L. (2001) Gene expression patterns of breast carcinomas distinguish tumor subclasses with clinical implications. *Proceedings of the National Academy of Sciences - PNAS*, 98 (19), 10869-10874.

Tung, N. & Garber, J. E. (2022) PARP inhibition in breast cancer: Progress made and future hopes. *NPJ Breast Cancer*, 8 (1), 47.

Ullah, F., Khan, T., Ali, N., Malik, F., Kayani, M., Shah, S. and Saeed, M., 2015. Promoter Methylation Status Modulate the Expression of Tumor Suppressor (RbL2/p130) Gene in Breast Cancer. *PLOS ONE*, 10(8), p.e0134687.

Vichai, V. & Kirtikara, K. (2006) Sulforhodamine B colorimetric assay for cytotoxicity screening. *Nature Protocols*, 1 (3), 1112-1116.

Vu, T. & Claret, F. X. (2012) Trastuzumab: Updated mechanisms of action and resistance in breast cancer. *Frontiers in Oncology*, 2 62.

Wang, L., Wu, C., Rajasekaran, N. & Shin, Y. (2019) Loss of tumor suppressor gene function in human cancer: An overview. *Cellular Physiology and Biochemistry*, 51 (6), 2647-2693.

Wang, S., Alpsy, A., Sood, S., Ordonez-Rubiano, S. C., Dhiman, A., Sun, Y., Jiao, G., Krusemark, C. J. & Dykhuizen, E. C. (2021) A potent, selective CBX2 chromodomain ligand

and its cellular activity during prostate cancer neuroendocrine differentiation. *Chembiochem : A European Journal of Chemical Biology*, 22 (13), 2335-2344.

Wu, S., Zhu, W., Thompson, P. and Hannun, Y., 2018. Evaluating intrinsic and non-intrinsic cancer risk factors. *Nature Communications*, 9(1).

Yang, J., Nie, J., Ma, X., Wei, Y., Peng, Y. & Wei, X. (2019) Targeting PI3K in cancer: Mechanisms and advances in clinical trials. *Molecular Cancer*, 18 (1), 26.

Yersal, O. & Barutca, S. (2014) Biological subtypes of breast cancer: Prognostic and therapeutic implications. *World Journal of Clinical Oncology*, 5 (3), 412-424.

Zhang, Y. & Martin, C. (2005) The diverse functions of histone lysine methylation. *Nature Reviews. Molecular Cell Biology*, 6 (11), 838-849.

Zheng, S., Lv, P., Su, J., Miao, K., Xu, H. & Li, M. (2019) Overexpression of CBX2 in breast cancer promotes tumor progression through the PI3K/AKT signaling pathway. *American Journal of Translational Research*, 11 (3), 1668-1682.

Zhuang, J., Huo, Q., Yang, F. & Xie, N. (2020) Perspectives on the role of histone modification in breast cancer progression and the advanced technological tools to study epigenetic determinants of metastasis. *Frontiers in Genetics*, 11 603552

